NUWC-NPT TM 932033

NAVAL UNDERSEA WARFARE CENTER DIVISION
NEWPORT, RHODE ISLAND

Technical Memorandum

LASER DOPPLER VELOCIMETRY INVESTIGATION OF TRANSIENT IMPELLER FLOW

Date: 3May 1993

Prepared by: Paul J. Lefebvre
Paul J. Lefebvre

Robert G. Gregory
Robert G. Grégory

Launcher Systems
Development Division
Launcher & Missile
Systems Department

Report Documentation Page

Form Approved
OMB No. 0704-0188

1. REPORT DATE	2. REPORT TYPE	3. DATES COVERED
03 MAY 1993	**Technical Memo**	**03-05-1993 to 03-05-1993**

4. TITLE AND SUBTITLE
Laser Doppler Velocimetry Investigation of Transient Impeller Flow

5a. CONTRACT NUMBER

5b. GRANT NUMBER

5c. PROGRAM ELEMENT NUMBER

6. AUTHOR(S)
Paul Lefebvre; Robert Gregory

5d. PROJECT NUMBER
A44100

5e. TASK NUMBER

5f. WORK UNIT NUMBER

7. PERFORMING ORGANIZATION NAME(S) AND ADDRESS(ES)
Naval Undersea Warfare Center Division,Newport,RI,02841

8. PERFORMING ORGANIZATION REPORT NUMBER
TM 932033

9. SPONSORING/MONITORING AGENCY NAME(S) AND ADDRESS(ES)
Office of Naval Research

10. SPONSOR/MONITOR'S ACRONYM(S)
ONR

11. SPONSOR/MONITOR'S REPORT NUMBER(S)

12. DISTRIBUTION/AVAILABILITY STATEMENT
Approved for public release; distribution unlimited

13. SUPPLEMENTARY NOTES
NUWC2015

14. ABSTRACT
Instantaneous, local velocity measurements at the inlet and discharge of a 1/3-scale transient-operation, submarine weapon ejection pump impeller were taken with a laser Doppler velocimeter. The impeller was tested in the Naval Undersea Warfare Center's Impeller Test Facility under simulated, full-scale, transient operating conditions. Measurement results are sufficient to define inlet and discharge transient boundary conditions for subsequent computational simulations. However, due to the very highly transient nature of the present tests, inadequate LDV measurement data rates precluded obtaining data near and between impeller blades.

15. SUBJECT TERMS
Transient Launcher Impeller Technology; submarine weapon ejection pump impeller

16. SECURITY CLASSIFICATION OF:			17. LIMITATION OF ABSTRACT	18. NUMBER OF PAGES	19a. NAME OF RESPONSIBLE PERSON
a. REPORT	b. ABSTRACT	c. THIS PAGE			
unclassified	**unclassified**	**unclassified**	**Same as Report (SAR)**	**48**	

ABSTRACT

Instantaneous, local velocity measurements at the inlet and discharge of a 1/3-scale, transient-operation, submarine weapon ejection pump impeller were taken with a laser Doppler velocimeter. The impeller was tested in the Naval Undersea Warfare Center's Impeller Test Facility under simulated, full-scale, transient operating conditions. Measurement results are sufficient to define inlet and discharge transient boundary conditions for subsequent computational simulations. However, due to the very highly transient nature of the present tests, inadequate LDV measurement data rates precluded obtaining data near and between impeller blades.

ADMINISTRATIVE INFORMATION

This memorandum was prepared under Project No. A44100, "Transient Launcher Impeller Technology," principal investigator P. J. Lefebvre (Code 8322), sponsored by the Office on Naval Research under the Advanced Launchers Project of the Submarine Technology Block Program.

The authors of this memorandum are located at the Naval Undersea Warfare Center Division, Newport, RI 02841-1708.

TABLE OF CONTENTS

LIST OF ILLUSTRATIONS

LIST OF ILLUSTRATIONS (Cont'd)

LIST OF TABLES

NOMENCLATURE

C_q	Flow Coefficient
Q	Volumetric Flow Rate (l/sec)
V_x	Annular Inlet Velocity (m/sec)
U	Impeller Tip Speed (m/sec)
N	Impeller Rotational Speed (RPM)
D	Impeller Blade Inlet Tip Diameter (cm)
d	Impeller Hub Diameter (cm)
C_h	Static Head Coefficient
H	Head Developed (m)
RPM	Impeller Rotational Speed (Used Interchangeably with N)
g	Acceleration Due to Gravity (m/sec^2)
Re_D	Inlet Pipe Reynolds Number
M	Number of Samples for Ensemble Averaged Data
$<I(t)>$	Ensemble Average of an Instantaneous Quantity I
RMS	Root Mean Square
$<I(t)_{RMS}>$	RMS Fluctuations About the Ensemble Average of I
d_f	Measuring Volume Fringe Spacing (μm)
N	Number of Fringes in Measuring Volume
d_m	Measuring Volume Diameter (mm)
l_m	Measuring Volume Length (mm)
λ	Light Wavelength (nm)
t	Time (seconds)

NOMENCLATURE (Cont'd)

r	Radial Position in Inlet Pipe or Test Section (cm)
R	Radius of Inlet Pipe Inner Wall (cm)
u_{cl}	Time-mean Velocity at Inlet Pipe Centerline (m/sec)
$u(t)_{cl}$	Instantaneous Velocity at Inlet Pipe Centerline (m/sec)
u	Time-mean Inlet Pipe Velocity (m/sec)
u'	Standard Deviation of u (m/sec)
U_1	Inlet Pipe Mean Velocity (m/sec)
$u(t)$	Instantaneous Axial Velocity Component (m/sec)
$<u(t)>$	Ensemble Averaged Instantaneous Inlet Pipe Velocity (m/sec)
$<u(t)_{RMS}>$	RMS Fluctuations About the Ensemble Averaged Velocity u(t) (m/sec)
$v(t)$	Instantaneous v-Velocity Component (m/sec)
$u_t(t)$	Instantaneous Tangential Velocity Component (m/sec)

1. INTRODUCTION

The pump impeller currently used on submarines to launch weapons operates under highly transient (i.e., accelerating and decelerating) conditions throughout the launch. To date, these impellers, along with those for other known transient applications, have been designed exclusively by applying quasi-steady analysis and design techniques and ignoring any potential transient effects. This approach amounted to assuming that, at any instant in time during a transient, all flow conditions (and, hence, pump performance) were identical to those during steady-state operation while operating at the instantaneous pump speed and flow rate. This approach was taken because little was known about the physics of transient impeller operation.

In an effort to understand the salient physics associated with the hydrodynamics and hydroacoustics of transient impeller operation, the Naval Undersea Warfare Center (NUWC) Division, Newport, RI developed its Impeller Test Facility (ITF). The facility is unique since, in addition to providing steady-state pump operation, it provides user-defined transient operation for the simulation of weapon launch from any submarine. Transient control is obtained through simultaneous control of both pump rotational speed and flow rate.

Recently completed studies conducted in the facility have evaluated both the hydrodynamic and cavitation performance of these submarine pump impellers. The transient hydrodynamic performance study is documented in Lefebvre and Barker [1]. Results showed that transient effects are significant. At the start of the transient, the head rise developed across the impeller is considerably higher than the quasi-steady value; this difference has been tentatively assumed to be associated with an impulsive pressure rise. After the effects of this impulsive pressure decay, the situation reverses and the quasi-steady assumption overestimates the actual transient head rise by as much as 37 percent. This reduced performance during the transient lasts for a significant duration around the time of peak rotational speed of the impeller.

Transient operation effects on impeller cavitation were also evaluated and results are presented in Lefebvre et al. [2]. Unlike hydrodynamic performance, transient cavitation characteristics, for the weapon launch transient, were shown to agree with the quasi-steady performance. This includes agreement in cavitation inception depth, type, and location of cavitation and also cavitation desinence as the impeller coasts to a stop.

The substantial effects observed on impeller hydrodynamic performance due to transient operation have demonstrated that the quasi-steady assumptions commonly used for the design of impellers that operate under transient conditions are not valid for many applications. Transient effects must be incorporated in the design process to improve performance prediction capabilities and to optimize designs.

To better understand transient effects and to eventually develop design methods and guidelines, the present study was initiated. The objective was to apply laser Doppler velocimetry (LDV) to define as much of the impeller transient flow field details as possible. Results are to be used during subsequent computational simulations to provide transient inlet and

outlet boundary conditions and to provide code validation data.

This technical memorandum reports details of the present study. The discussion includes experimental procedures and presentation of results.

2. EXPERIMENTAL FACILITY

All experiments were conducted at the Naval Undersea Warfare Center's Impeller Test Facility (ITF). A brief description of the facility is provided in this section of the document. More detail can be found in Gregory et al. [3].

IMPELLER TEST FACILITY

Control systems for transient operation have been developed that operate simultaneously in order to produce user-specified impeller rotational speed (N) and flow rate (Q) time histories. Simultaneous control of these variables provides a means of maintaining the desired time history for the parameter being modeled -- the flow coefficient C_q, which is defined as

$$C_q = \frac{V_x}{U} \quad \alpha \quad \frac{\frac{Q}{\pi(D^2 - d^2)/4}}{\frac{\pi N D}{60}}, \tag{1}$$

where D is the blade inlet tip diameter, d is the hub diameter, V_x is the annular inlet velocity, and U is the impeller tip speed at the inlet and is proportional to $N \cdot D$.

The layout of the ITF is shown in figure 2-1. The facility is a closed-loop recirculating system. The impeller under test is housed in the test section, which was designed to simulate the near impeller flow field of an actual submarine impulse tank. The impulse tank is designed to accommodate a wide range of impellers and the addition of a diffuser or collector at the impeller discharge if required in the future. No diffuser was used during the present study.

Figure 2-2 shows a schematic of the impeller used for this investigation; figure 2-3 is the corresponding steady-state hydrodynamic performance curve expressed as C_h vs. C_q where

$$C_h = \frac{gH}{N^2D^2} \ . \tag{2}$$

H is the head developed by the pump (the pressure rise across the impeller), and g is the acceleration due to gravity. Data are shown for a range of impeller speeds and a least

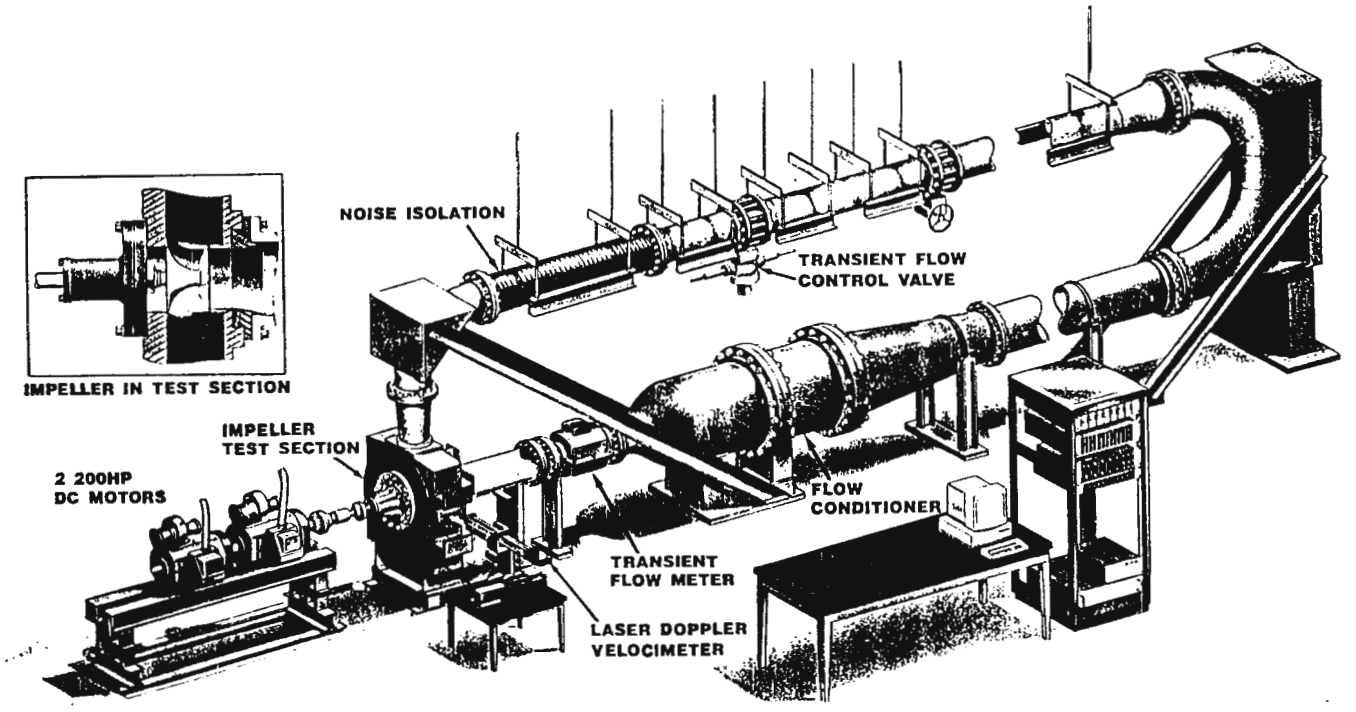

Figure 2-1. NUWC Impeller Test Facility

squares curve fit of all the data is plotted as the solid line. The collapse of data onto a single curve for the different impeller speeds and the small amount of scatter provides confidence in the facility and associated instrumentation.

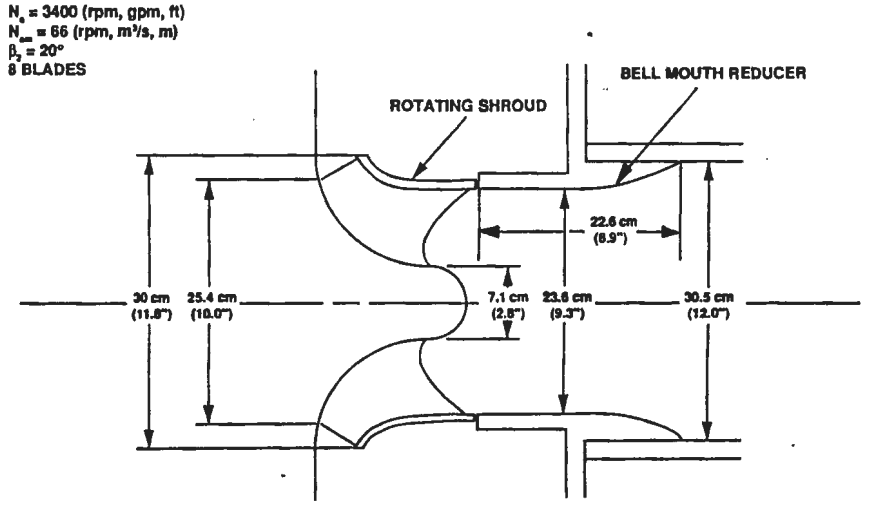

Figure 2-2. Schematic of 1/3-Scale Impeller

Visual access for flow visualization and laser Doppler velocimeter (LDV) measurements at the impeller discharge is obtained through a 7.62-cm (3-in.) by 17.78-cm (7-in.) viewing port on the side of the test section. The inlet flow to the impeller is through a 30.48-cm-diameter (12-in.) clear cast acrylic pipe that allows visual access to the blades' leading edge. Photographs of the test section including the visual access areas of the facility are shown in figures 2-4 and 2-5.

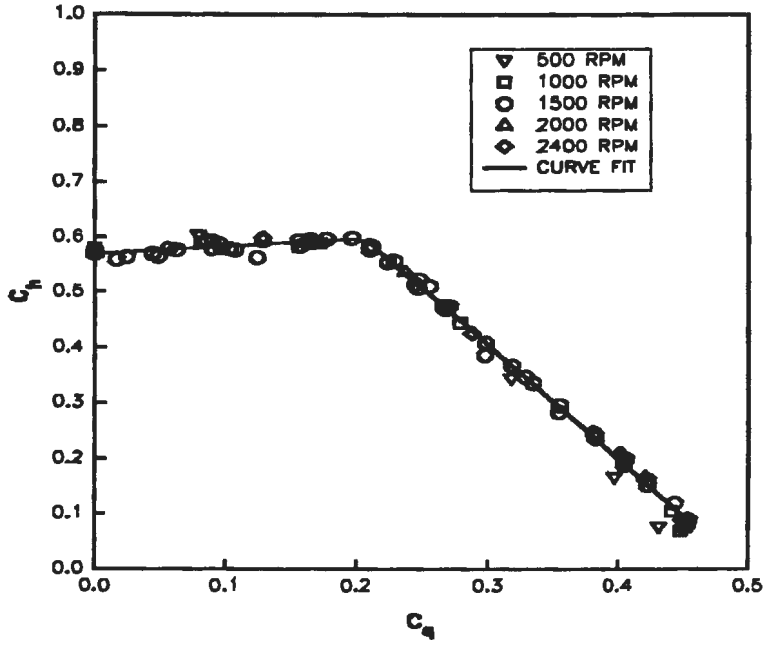

Figure 2-3. Steady-State Impeller Performance

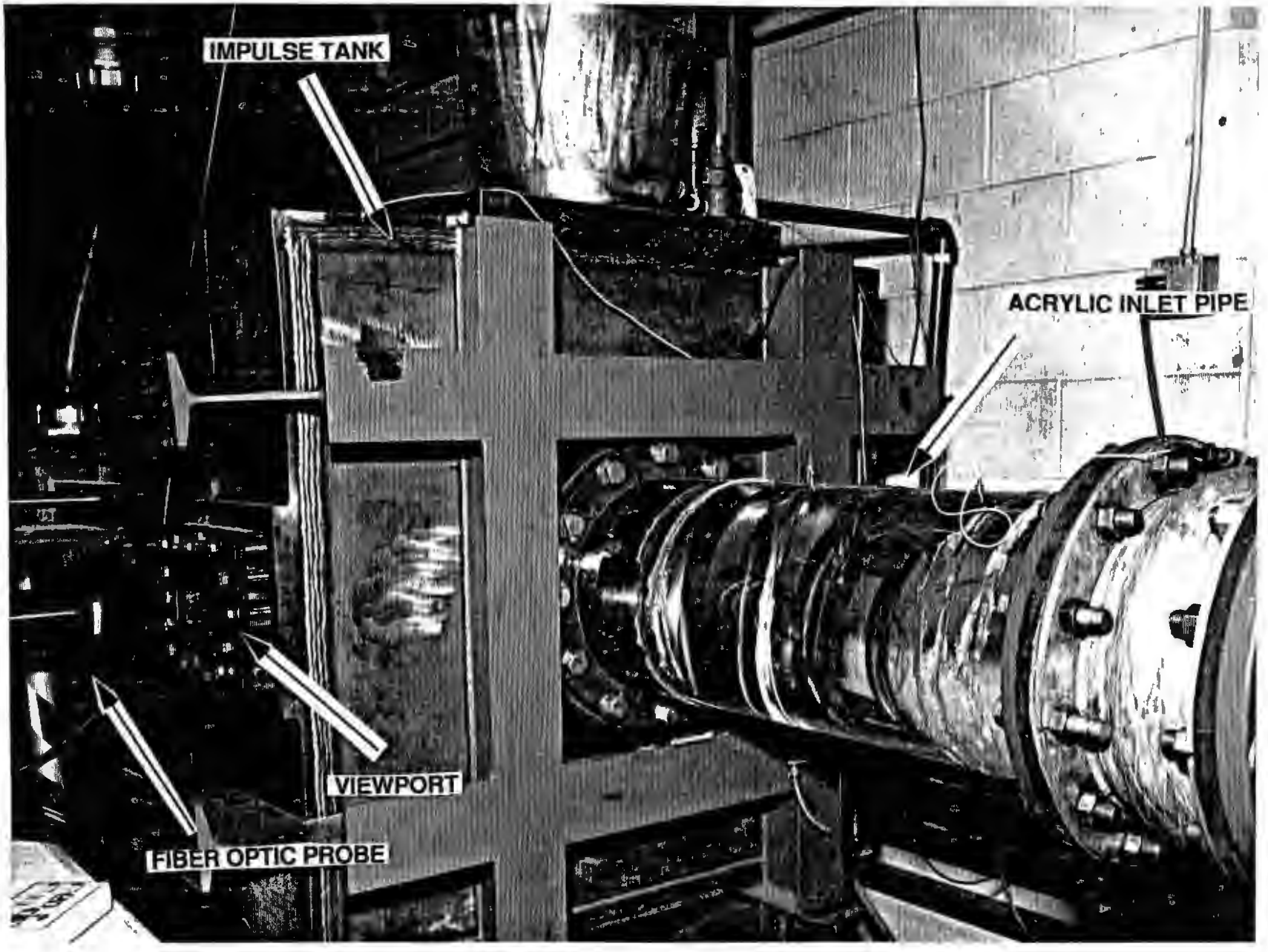

Figure 2-4. Inlet Side of Test Section

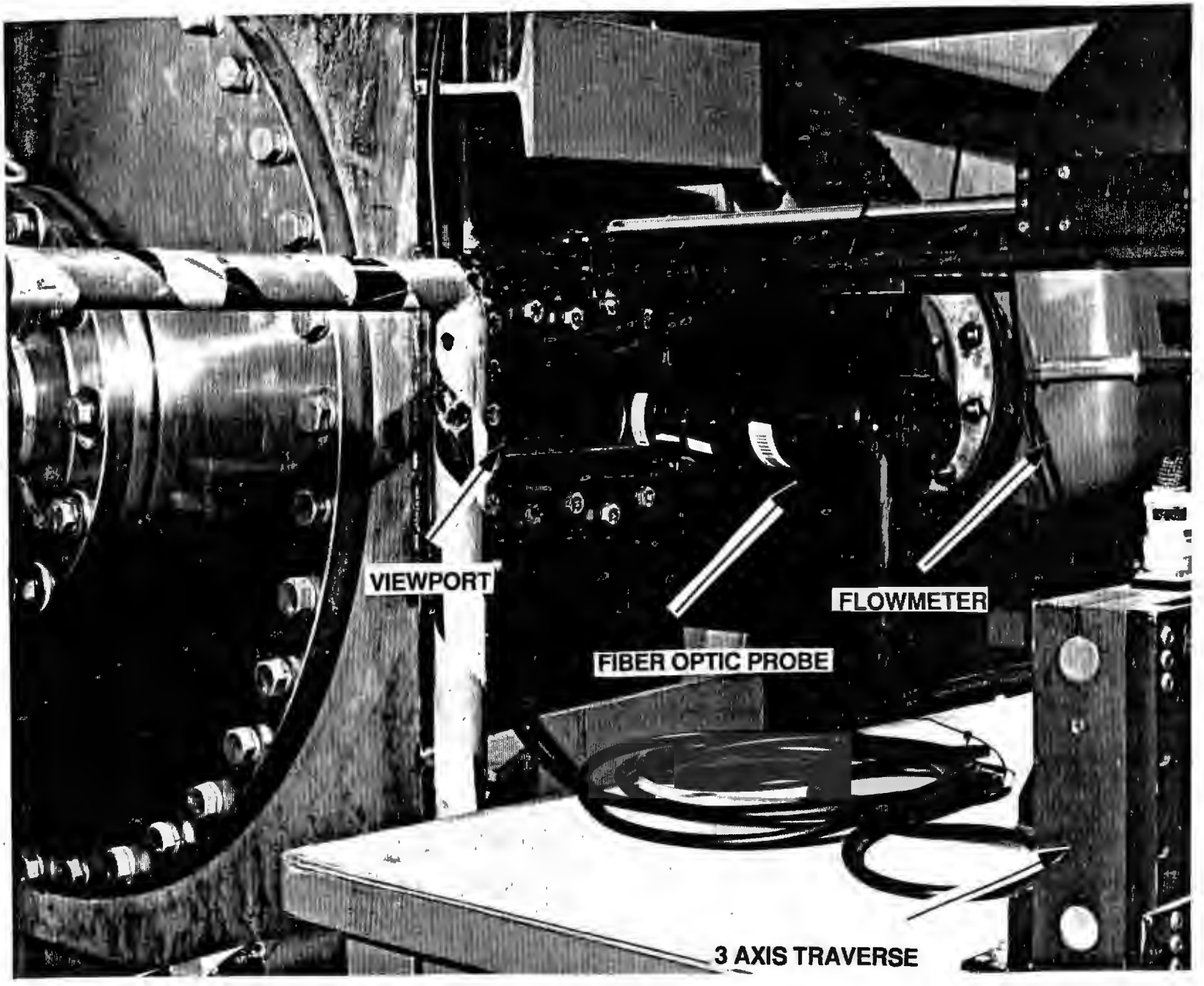

Figure 2-5. Discharge Side of Test Section

The flow into the inlet pipe is conditioned by a 91.44-cm-diameter (36-in.) settling tank and nozzle with 15.24-cm-long (6-in.), 0.635-cm-cell (1/4-in.) size honeycomb sandwiched between each of the two flanges at the settling tank. The resulting flow at the inlet pipe entrance has a velocity profile uniform within 1.0 percent across its diameter and a turbulence intensity of less than 1.0 percent.

The flow in the facility is developed by the test impeller, which is powered by two General Electric, 200-hp, low-inertia, DC electric motors connected in series. The instantaneous rotational speed of the motors is controlled by a dedicated microprocessor-based feedback control system that has both steady-state and transient operating capabilities. The feedback signal is the rpm from a tachometer mounted on the motor shaft at the rear of the motors. The command signal, whether one constant value of rpm for steady-state operation or a file of rpm vs. time for transient operation, is downloaded from an IBM-compatible PC to the microprocessor controller. The PC is used for all interfacing with the controller, including setting of all safety and operational parameters.

Flow rate is controlled by a second control system that governs the motion of the 40.64-cm-diameter (16-in.) control valve installed downstream of the test section. The feedback signal is the valve position as measured by a position indicator mounted on the valve stem. The command signal is generated by a second IBM-compatible PC. This control system operates in either steady-state mode or transient mode; for the latter, a transient valve position time history affords transient flow rate control. This PC also controls initiation of all events, including gating of data acquisition hardware and triggering of the motor control system.

A second 40.64-cm-diameter (16-in.) valve is installed downstream of the control valve. This manually actuated valve is used to "load" or add additional hydrodynamic losses in the facility. In this way, the pressure drop required in the facility to control flow rate is accomplished across both the manual and the transient valve, resulting in reduced noise and a lower susceptibility to cavitation than if the total pressure drop occurred over just one valve. During a transient run, the manual valve is set to a stationary position chosen to provide an optimum pressure drop distribution across each of the valves.

To reduce structural and fluid-borne noise, vibration and noise isolators are used where appropriate. The water in the facility is conditioned by use of a deaerator, a filter (1 to 25 microns), and a heat exchanger. Provision is included for conducting tests at facility pressures ranging from a slight vacuum up to a gauge pressure of 758,500 pascals (110 psig). (In this study all tests, steady-state and transient, were conducted at facility pressures sufficiently high to preclude cavitation.)

TRANSIENT PROFILE

The transient profiles for impeller rotational speed and flow rate used during these tests are given in figure 2-6. As shown, the impeller is accelerated from rest followed by a period of deceleration. The peak flow rate was 321 l/sec (5130 gal/min), resulting in a peak velocity in the 30.48-cm-diameter (12-in.) inlet pipe of 4.6 m/sec (14.6 ft/sec). The peak rotational speed of 2400 rpm was reached within 0.4 second from the start of the transient. Once peak rotational

speed was reached, at approximately 0.45 second, controlled impeller deceleration was immediately initiated. At 1.05 seconds, power to the motors was terminated and the motors coasted to a stop. The complete transient, including deceleration, lasted approximately 2.5 seconds. For weapon launch applications, the main region of interest is from initiation of the transient to peak Q at approximately 0.65 second, which corresponds to weapon exit from the launch tube.

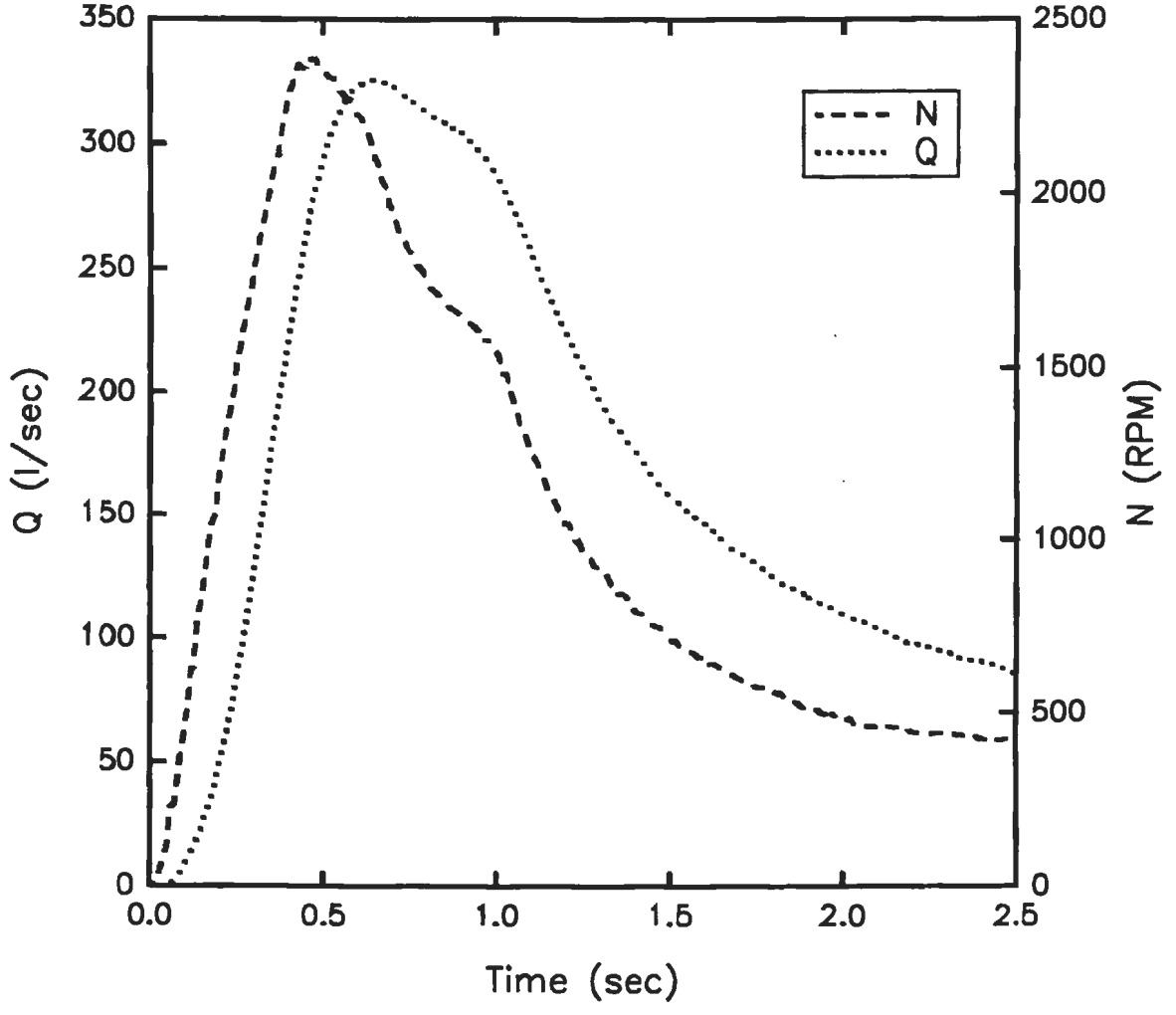

Figure 2-6. Flow Rate and Pump Rotational Speed Time Histories

The high level of acceleration in both N and Q during the early portion of the transient should be noted. For a considerable portion of the ramp-up, each variable experiences an approximately constant acceleration with values of 720 rad/sec^2 and 0.9 g for N and Q, respectively. The resulting transient C_q time history, shown in figure 2-7, is an indication of incidence angle at the blade leading edge and also its time rate of change.

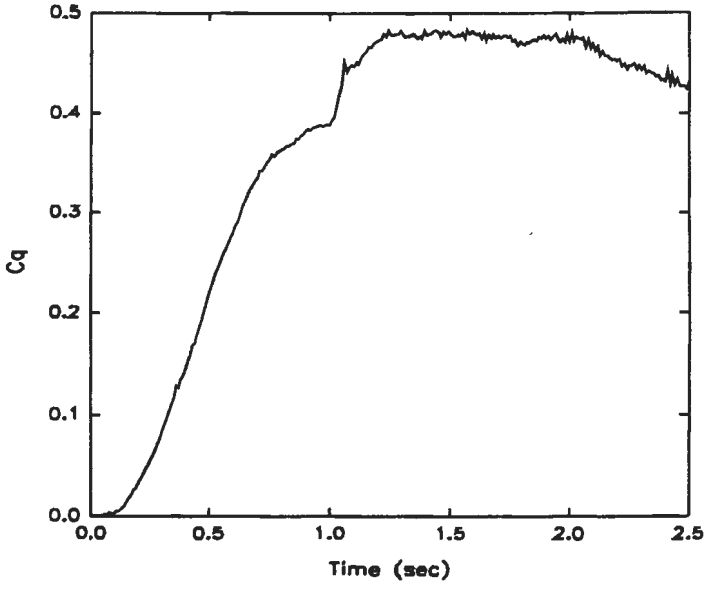

Figure 2-7. C_q versus Time

For reference, figure 2-8 shows the inlet pipe Reynolds number, $Re_D = D_1U_1/\upsilon$, versus time for this transient, where D_1 is the inlet pipe diameter, U_1 is the mean inlet pipe velocity, and υ is the fluid's kinematic viscosity.

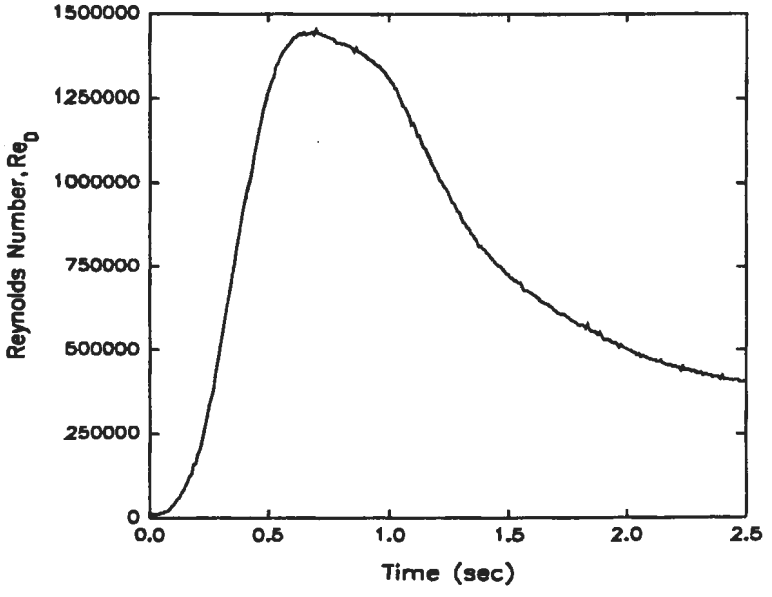

Figure 2-8. Inlet Pipe Reynolds Number

An ensemble average of the inlet pipe mean velocity from 30 transient test runs is shown in figure 2-9. The ensemble average for an instantaneous quantity I at time t is

$$< I(t) > = \frac{1}{M} \sum_{i=1}^{M} I(t)_i \quad , \tag{3}$$

where < > denotes the ensemble-averaged quantity, and M = 30 for the present study.

From this ensemble average a determination as to the ability of the facility to repeat a given transient history can be made. Figure 2-10 shows the standard deviation (RMS) versus time curve for the aforementioned 30 runs, non-dimensionalized by the instantaneous ensemble averaged velocity.

The RMS fluctuations of I about its ensemble average were calculated according to the relationship

$$< I(t)_{rms} > = \frac{1}{M} \sqrt{\sum_{i=1}^{M} I(t)_i^2 - < I(t) >^2} \quad . \tag{4}$$

In the results section of this report, the RMS values of axial velocity were used as a measure of (instantaneous) turbulence intensity.

Facility repeatability, at a 95% confidence level, can be obtained by taking plus or minus two standard deviations. Figure 2-10 shows that from startup to 0.22 second (while the flow is low) the non-repeatability decreases from ±20 percent to ±3.0 percent. Repeatability error is less than 3.0 percent from 0.22 second to 1.07 seconds, which corresponds to the main portion of the acceleration and beginning deceleration period of the transient event. In fact, from 0.40 to 1.05 seconds the RMS is 0.5 percent, resulting in a repeatability error of less than 1 percent and indicating a very repeatable flow. At 1.05 seconds the motor power is terminated and the repeatability deteriorates due to the uncontrolled coasting down of the flow.

Since facility repeatability during the main region of interest of the transient, 0.22 to 1.05 seconds, is within ±3.0 percent, for the purpose of the current test program differences between runs is considered negligible. Therefore, even though the various data were collected over many runs, they can be considered as taken over a single run with various results at any instant in time considered coincident in real time.

3. INSTRUMENTATION

Pump hydrodynamic performance was obtained through measurements from an instrumentation suite that included a transient flowmeter, four high frequency response pressure sensors, a torque meter, a tachometer, and an optical encoder. Sensor locations are given in figure 3-1, while model numbers and pertinent operational data are listed in table 3-1. Stated accuracy values are for the measurement and not the sensor alone since the values include propagation of errors from the signal conditioning and data acquisition hardware.

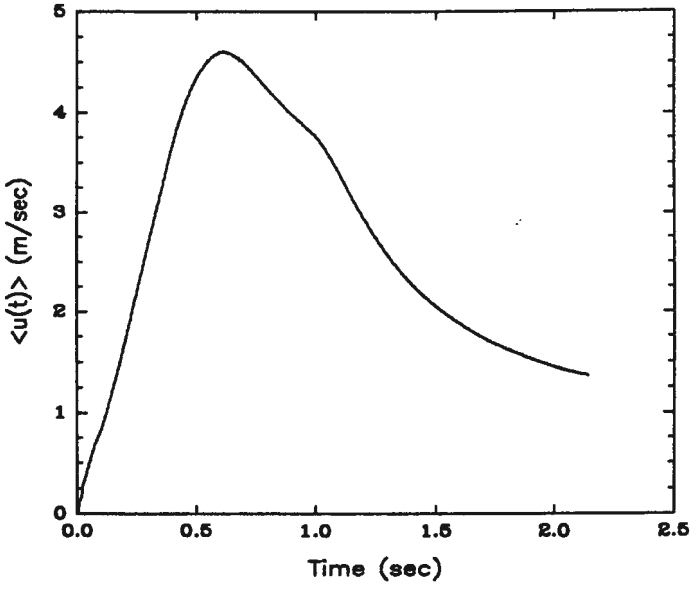

Figure 2-9. Ensemble-Averaged Inlet Pipe Velocity Time History from 30 Repeat Runs

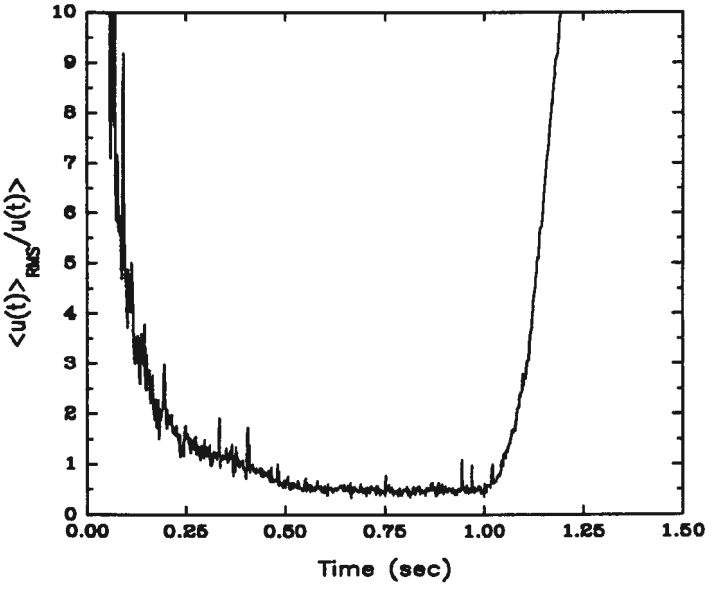

Figure 2-10. $\langle u(t)_{RMS}/u(t)\rangle$ versus Time

The transient flowmeter, described in Lefebvre and Durgin [4], measures the instantaneous flow rate to within ±1 percent of reading accuracy in either steady-state or transient operation. This meter is an electromagnetic flowmeter that, inherently, doesn't obstruct the flow. Additionally, since the meter averages the flow over the pipe cross-section, measurements are insensitive to velocity profile. This is an important attribute for transient flow applications since the velocity profile may change throughout the transient.

Inlet pressure was monitored by high-frequency-response, flush-mounted pressure transducers installed in the inlet pipe at one and two pipe diameters upstream of the impeller nose. Discharge pressure was measured with two similar transducers placed in the test section. The first sensor was mounted at the top of the test section, while the second was located on the side opposite the side viewing port at an elevation equal to that of the inlet pipe centerline. These sensors allowed for the identification of any asymmetry in the discharge flow field.

The remaining sensors are of standard design and the applications here are typical. Therefore, no further discussion of these sensors is provided. Calibration procedures for all sensors and instrumentation are described in detail in Lefebvre and Barker [1] and are not repeated here.

A MASSCOMP 6600 Data Acquisition System was used to digitize and acquire all hydrodynamic performance data. The MASSCOMP can acquire both digital and analog data with a maximum total throughput rate of 1 MHz.

The LDV hardware used during this study consisted of a Lexel Model 95-4 argon-ion laser, a TSI Model #9100-7 optics system reconfigured with a 50-m-long fiber optic cable and TSI model #9275 fiber optic probe. The LDV processor was a TSI IFA 550 Intelligent Flow Analyzer processor interfaced through a 386-20-MHz IBM-compatible PC. The fiber optic probe was mounted on a three-axis TSI Model 9400 auto-traverse.

Two focusing lenses were used for this investigation. The first was a Model #9167-350 lens with a focal length of 350.6 mm (13.80-in.) and a half angle of 3.971 degrees. The second was a Model #9118-250 lens with a focal length of 249.5 mm (9.82-in.) and a half angle of 5.525 degrees. The 350.6-mm lens was used for all inlet testing, both steady-state and transient, where the longer focal length was required to obtain data across the 30.48-cm (12-in.) inlet pipe. The 249.5-mm lens was used for discharge testing where the smaller measuring volume dimensions provided a decrease in phase noise, which in turn allowed for deeper penetration of the discharge flow field than would have been possible with the longer focal length lens.

Table 3-1. Instrumentation

USE	HARDWARE	RANGE	ACCURACY	SIGNAL COND.
Pressure	Flush Mounted: Kulite XTM-190-100	0.0 - 2.8 MPa	+/- 0.7 % of reading 0 - 80 kHz	Ectron 563 FL
Temperature	Cole-Palmer R8415-24 Thermister Probe	0.0 - 120.0 °C	+/- 0.05 °C	Cole-Palmer R8502-50
Transient Flow Rate	Foxboro Magnetic Flow Body with NUWC Electronics	0.0 - 40.0 ft/sec	+/- 1.0 % of reading	NA
Impeller Speed (rpm)	Radio-Energie Type RPY444RICB/YA Tachometer & Burton Mentor 55R Controller	0 - 2400 rpm	+/- 2 rpm	NA
Impeller Rotational Position	Dynapar Model 63-C-ADF-0900-AO Optical Encoder	0 - 360 degrees	+/- 0.1 degree	C-Tek Model # LIN-101-41-11-41-B Pulse Counter
Laser Doppler Velocimetry	TSI model IFA 550 Signal Processor with Fiber optic Probe	0 to 15 MHz Doppler Frequency	+/- 1.5%	NA
Recorders	Masscomp 6600 Computer With Removable Hard Drive	NA	16 bit A-D	NA

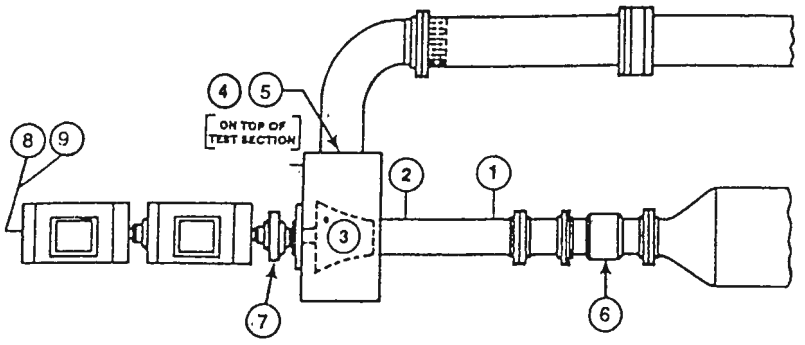

LOCATION	SENSOR
1 - 4	Flush Mounted Pressure Transducer
5	Thermister Probe
6	Transient Flowmeter
7	Torquemeter
8	Optical Rotary Encoder
9	Tachometer

Figure 3-1. Instrumentation Locations

Table 3-2 gives the important measuring volume characteristics for each of the aforementioned focusing lenses.

Table 3-2. Measuring Volume Characteristics

	Green Beam (λ = 514.4 nm)		Blue Beam (λ = 488.0 nm)	
	9118-250	9167-350	9118-250	9167-350
Fringe Spacing d_f, μm	2.672	3.715	2.534	3.523
Number of Fringes, N_{fr}	23.6	24.0	23.7	23.8
Measuring Volume Diameter, d_m, mm (in.)	0.063 (0.0025)	0.089 (0.0035)	0.060 (0.0024)	0.084 (0.0032)
Measuring Volume Length, l_m, mm (in.)	0.651 (0.026)	1.282 (0.050)	0.620 (0.024)	1.210 (0.0476)

Table 3-3 provides uncertainty estimates for the test data or calculated parameters.

Table 3-3. Measurement Accuracy of Final Parameters

Parameter	Uncertainty
Flow Rate, Q	+/- 1.0 %
Impeller Rotational Speed, N	+/- 1.0 %
Head, H	+/- 2.0 %
Head Coefficient, C_h	+/- 4.0 %
Flow Coefficient, Cq	+/- 4.0 %
Time, t	+/- 60 msec

4. OPERATIONAL PROCEDURES

This section of the report presents the test procedures implemented during both the transient and steady-state operation of the Impeller Test Facility for this investigation. The first subsection discusses general procedures that are common to both test modes. Procedures that are particular to only steady-state or transient operation are described in their respective sections. The transient operation section is further divided into inlet and discharge testing procedures.

GENERAL

The preliminary operational procedures for the Impeller Test Facility encompass the use of the facility hardware as well as the filtering and deaeration system. Prior to testing, the facility was filled with tap water (approximately 1500 gallons), which was filtered to 10 microns. Filtration of the facility's water supply is especially critical to LDV testing due to the small size of the seed particles (less than 5 microns) and the decreased signal-to-noise ratio (SNR) caused by particles in unfiltered water. After the facility had been filled, the water was deaerated and recirculated through the 10-micron filters for a period of 12 hours to ensure water quality. Prior to LDV testing, the traverse unit holding the fiberoptic probe was both leveled and checked for perpendicularity to the viewport or pipe. This ensured that there would be no unpredicted beam refractions due to the probe being off axis in any plane. Just prior to all testing the facility was pressurized via a hydropump to a level sufficient to eliminate the possibility of cavitation, which could lead to impaired impeller performance and/or the generation of cavitation bubbles that could interfere with LDV measurements close to the impeller.

STEADY-STATE TEST PROCEDURE

Steady-state testing was conducted on the inlet to the impeller through the 30.48-cm clear acrylic pipe described in section 2. Both u- and v-components (axial and vertical, respectively) of the flow were acquired. The main reason for acquiring the v-component was to identify any asymmetries or fluctuations in the flow. If turbulent Reynolds stress measurements were the main interest, the radial flow component would have been acquired; pipe curvature and index of refraction effects make that measurement almost impossible. Table 4-1 gives the description, position, and important operational parameters of each series of tests. The radial position shown (r/R) is the non-dimensionalized pipe radius with r/R = 0 at the pipe centerline. The position upstream of the impeller is defined as the axial distance from the nose of the impeller to the point on the inlet pipe where measurements were made.

The impeller rotation speed (N) in column 4 was controlled with the motor control system. The desired flow rate, and hence the desired C_q, was established using the 40.64-cm control and manual loading valves. The output of the steady-state Foxboro flowmeter electronics was monitored using a voltmeter until the correct flow rate was attained. Once achieved, the facility

maintained this operating condition for the duration of testing with negligible fluctuations. Next, the titanium dioxide flow seeding particles were added until the steady-state data rate was maximized as observed on the IFA 550 processor with the measuring volume at r/R = 0.667 (10.16 cm (4-in.) from the pipe centerline). The typical maximum data rate was on the order of 2 to 3 kHz. For the steady-state tests the green beams were used for the u-component of flow and the blue for the v-component. As mentioned in section 3, the 350.6-mm focal length lens was used for this phase of the investigation.

Table 4-1. Steady-State Test Matrix

Test Description	Position Upstream of Impeller	Radial Position (r/R)	N (rpm)	Flowrate [l/s,(gal/min)]	Flow Coefficient (C_Q)
Velocity Profile	3 Diameters	0 to 1	500	57.4 (910)	0.23
Velocity Profile	3 Diameters	0 to 1	1500	172.2 (2730)	0.23
Velocity Profile	2 Diameters	0 to 1	500	57.4 (910)	0.23
Velocity Profile	2 Diameters	0 to 1	1500	172.2 (2730)	0.23
Velocity Profile	1 Diameter	0 to 1	500	57.4 (910)	0.23
Velocity Profile	1 Diameter	0 to 1	1500	17.2 (2730)	0.23
Velocity Profile	1 Diameter	0 to 1	1500	37.5 (594)	0.05
Velocity Profile	1 Diameter	0 to 1	1500	74.9 (1187)	0.10
Velocity Profile	1 Diameter	0 to 1	1500	112.3 (1780)	0.15
Velocity Profile	1 Diameter	0 to 1	1500	224.6 (3560)	0.30
Velocity Profile	1 Diameter	0 to 1	1500	299.5 (4747)	0.40
Time History	1 Diameter	0.667	500	74.9 (1187)	0.10

For steady-state velocity profile measurements, data were acquired starting at the pipe centerline (r/R = 0) and ending as close to the pipe inner wall as possible (typically 13.97 to 14.61 cm (5.50 to 5.75 in.) from the centerline). Data were acquired as close to the inner wall as possible, i.e., until reflections degraded the SNR to the point where the LDV processor was unable to identify the Doppler signal. The IFA 550 Intelligent Flow Analyzers were used to acquire data. The Model 9400 traverse was programmed through the TSI FIND software to automatically traverse the pipe in 1.27-cm (0.5-in.) increments up to 12.7-cm (5-in.) from the centerline, then in 0.635-cm (1/4-in.) increments for the remaining points. At each radial position, enough data were collected to ensure that proper statistical parameters were met.

Due to pipe curvature and index of refraction effects, the u- and v-component measurement volumes were not coincident for most radial positions. Reynolds stress turbulence measurements were therefore not possible. However, turbulence intensity, u', was obtained for the u-component. Additionally, following a u-component measurement, the LDV probe had to be moved so that the v-component measurement could be taken at the same radial position as the complementary u-component. For the v-component of the flow, a ray tracing computer code was written to calculate the probe position required to acquire v-component data at the same points as u-component data.

For time history examinations of the steady-state flow to quantify flow unsteadiness, the probe was positioned so that data were acquired at r/R = 0.667. For this test the facility was set to a low C_q to examine the effects of off-design flow on the inlet flow field. Data for both u- and v-components were acquired for 20 seconds in order to later generate a time history for analysis.

TRANSIENT TEST PROCEDURE

Investigations of both the impeller inlet and discharge transient flow fields were conducted. For both regions, the 514.5-nm wavelength green beam was used for all testing. The substantially higher power output of the green beams over that of the blue was needed to increase the SNR and acquire data at a sufficient rate during the high acceleration of the transient event. During that portion of the transient, the axial flow accelerates from 0 to 4.6 m/sec (14.6 ft/sec) in 0.7 second in the inlet pipe and the discharge tangential velocity reaches 27.4 m/sec (90 ft/sec) during the same time span. Again, the flow seeding particle was titanium dioxide. The facility control system, as described in section 2, allowed for the input of user-defined impeller rotational speed and control valve time histories to accurately model a weapon launch transient.

Inlet Flow

All inlet transient testing was conducted at axial positions one and two pipe diameters (30.48 cm and 60.96 cm.) upstream of the impeller nose. Transient measurements were made at each of the radial stations used for the steady-state tests. At each of these positions, flow rate data from the NUWC-developed transient flowmeter and impeller rotational speed (rpm) were acquired on the MASSCOMP 6600 while LDV data were acquired on the LDV 386 PC. The IFA 550's high pass and low pass filters were set to 30 kHz and 3 MHz, respectively, which enabled the processor to acquire velocity data from 0.11 to 11.14 m/sec (0.37 to 36.56 ft/sec). The processor's time-out function was set to 20 seconds to allow for acquisition of the full transient event. The lens used was the one with the 350.6-mm focal length.

To ensure proper data correlation with a common time reference, it was necessary to gate the IFA 550 processors with the rest of the facility control and data acquisition systems. This was accomplished in the following manner: LDV velocity data are transferred in real time from the IFA 550 to the Tandon 386-20 PC through the MI-550 Master Interface Board. This board, which is housed in the IFA-550, is responsible for the DMA (Direct Memory Access) data transfer from the IFA 550 to the PC. This interface has a 50-pin J24 connector that is used for DMA. Pins number 19 and 20 of this connector are an external synchronization for the MI-550 and IFA 550. If this external synchronization is triggered, the Time Between Data (TBD) bit #15 in word A of the digital data sent from the IFA 550 to the PC is reset. The external synchronization can be triggered by a positive TTL pulse of 1 μsec or greater. When this occurs, it gives a "time zero" or common time reference point for LDV data. The 5-volt output signal from the IBM AT valve controller, which controls the initiation of the transient and data acquisition on the MASSCOMP 6600, can be and is used as the trigger signal to the LDV hardware.

Discharge Flow

Investigation of the discharge flow field of the impeller transient was conducted through the rectangular viewport shown in figure 2-3, utilizing the 249.5-mm lens for the reasons given in section 3. Data were acquired at three radial positions measured radially from the outer impeller radius with $r = 0$ referenced to this point. At each of these radial positions, data were acquired at four axial (x) locations. The $x = 0$ position was at the upstream edge of the impeller discharge as

shown in figure 4-1. Table 4-2 shows important test parameters utilized for this phase of the investigation. Analog flow and pump rotational speed, along with digital impeller rotational position data, were acquired on the MASSCOMP 6600. Gating of the IFA 550 processors was the same as for the inlet transient tests

Table 4-2. Discharge Transient Test Matrix

Test Description	Radial Position cm (in.)	Axial Test locations - 4 positions cm (in.)	N (RPM)	Flow Rate [l/s,(gal/min)]	Flow Coefficient (Cq)
Time History	28.1 (11.0)	1.91, 0.0, -2.22, -3.18 (0.75, 0.0, -0.875, -1.25)	0-2400	0-321 (0-5130)	0-0.45
Time History	33.0 (13.0)	1.91, 0.0, -2.22, -3.18 (0.75, 0.0, -0.875, -1.25)	0-2400	0-321 (0-5130)	0-0.45
Time History	38.1 (15.0)	1.91, 0.0, -2.22, -3.18 (0.75, 0.0, -0.875, -1.25)	0-2400	0-321 (0-5130)	0-0.45

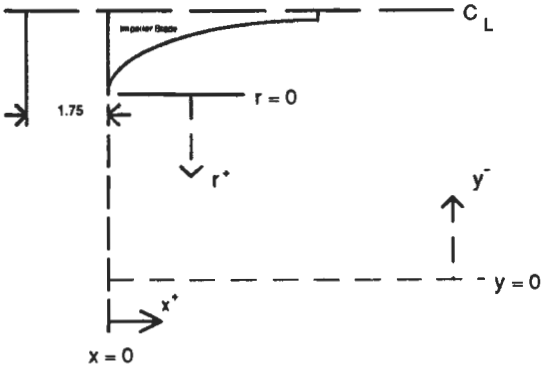

Figure 4-1. Discharge Test Schematic

5. RESULTS

STEADY-STATE IMPELLER, INLET PIPE DATA

Figures 5-1 through 5-4 show velocity profiles and turbulence intensity measurements for the impeller inlet pipe with the impeller operating at the design C_q of 0.23. The data in figures 5-1 and 5-2 were acquired at Re_D of 3.0×10^5, while the data in figures 5-3 and 5-4 were acquired at Re_D of 9.7×10^5. Velocity profiles are non-dimensionalized with the centerline velocity while $u' = u_{RMS}/u$.

Figure 5-1 shows the velocity profiles for one, two, and three pipe diameters upstream of the impeller nose at Re_D of 3.0×10^5. At both two and three diameters upstream of the impeller the flow is essentially uniform from r/R = 0 to 0.8. The difference between the profiles of these two locations is well within the accuracy of the LDV. When comparing these experimentally obtained velocity profiles with the law of the wall profile for fully developed flow it is obvious that the inlet flow is not fully developed. This was intentional in the facility design since the short inlet pipe is immediately downstream of the nozzle, which provides essentially uniform flow at its exit. This is assumed to be close to ship conditions since the actual inlet pipe is on the order of 7 pipe diameters long, substantially shorter than the approximate 35 pipe diameters required to achieve fully developed flow at this Reynolds number.

It can be seen that at these relatively low Reynolds numbers the effects due to the proximity of the bellmouth to the test station one diameter upstream of the impeller results in a more pronounced viscous layer in the flow. The velocity profile shows that the boundary layer has grown to such an extent that the flow is uniform only from r/R = 0 to 0.4. From figure 2-2 it can be seen that the leading edge of the bellmouth reducer is only 7.87 cm (3.1 in.) from the one diameter axial position.

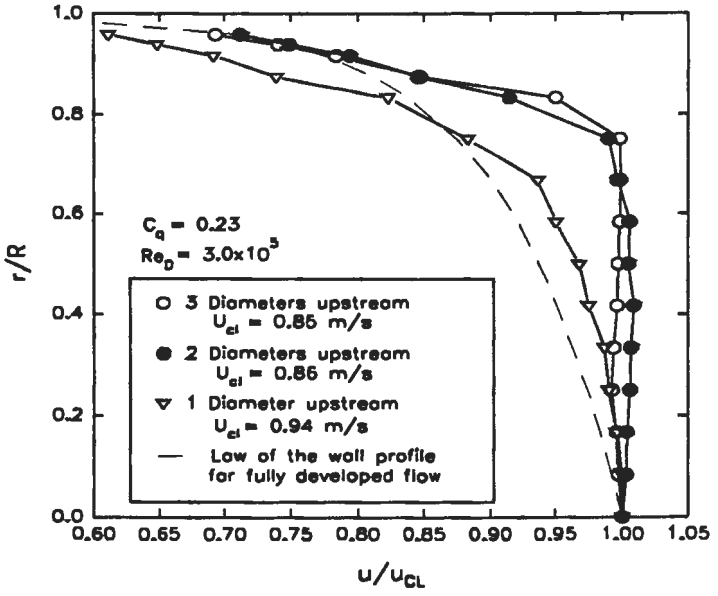

Figure 5-1. u-Component Velocity Profiles for Re_D of 3.0x10^5 and C_q of 0.23

A plot of turbulence intensity for the velocity profile shown in figure 5-1 is shown in figure 5-2. The turbulence intensity from r/R = 0 to 0.70 (uniform flow area) has a very low value of approximately 1 percent for all three axial positions. The actual turbulence intensity is potentially lower than 1 percent since the results are at the accuracy limits of the LDV. From r/R = 0.7 to r/R = 1.0 the turbulence intensity increases in the viscous (boundary) layer and is quantitatively in the range expected for such a flow.

Figure 5-3 shows the velocity profiles for one, two, and three pipe diameters upstream of the impeller nose at Re_D of 9.7x10^5. It can clearly be seen that at this higher Reynolds number the effect of the bellmouth reducer that was evident in the velocity profile one diameter upstream of the impeller (as seen in figure 5-1) is negligible. It is seen here that the velocity profiles at one, two, and three diameters upstream of the impeller are uniform within 3 percent from r/R = 0.0 to 0.70. As was the case for the lower Reynolds number flow from figure 5-1, the profiles two and three diameters upstream of the impeller are uniform within 1 percent for r/R = 0.0 to 0.7. The slight deviation of the one-diameter profile can be attributed to the slight effect of the bellmouth. Again, the difference between the experimental velocity profiles and the law of the wall profile for fully developed flow is due to the lack of sufficient entrance length for the inlet flow to fully develop.

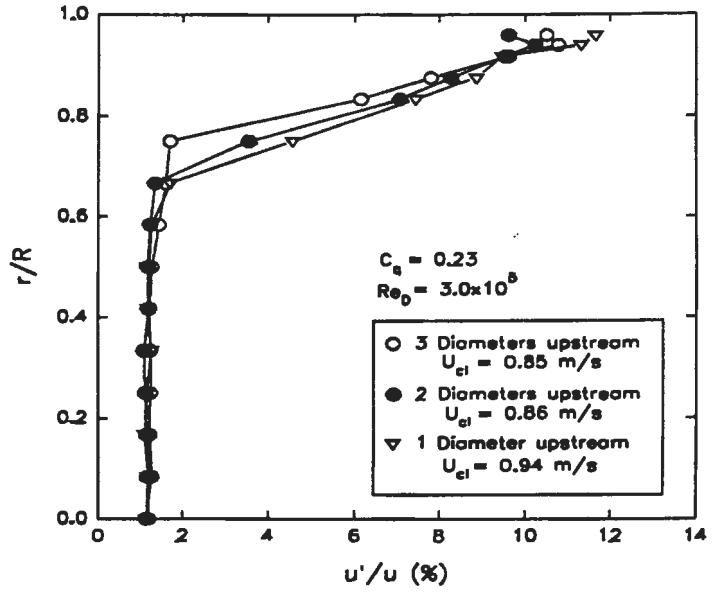

Figure 5-2. Turbulence Intensity for Re_D of 3.0x10^5 and C_q of 0.23

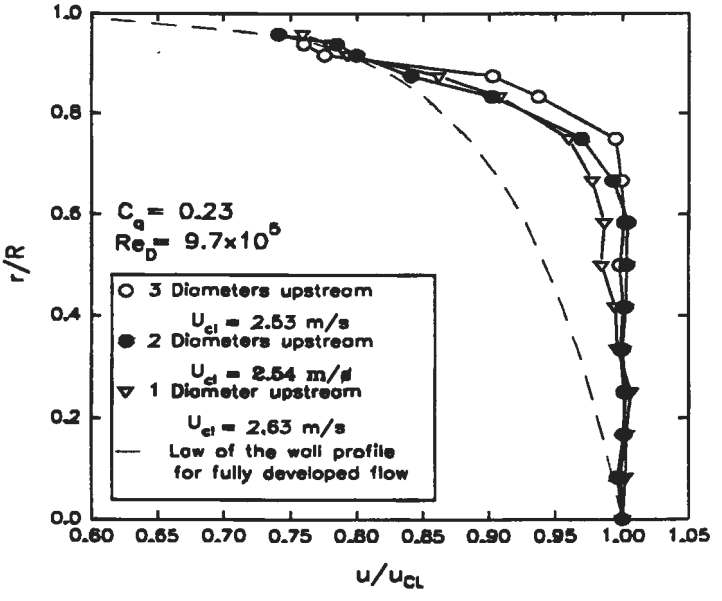

Figure 5-3. u-Component Velocity Profiles for Re_D of 9.7x10^5 and C_q of 0.23

A turbulence intensity plot for the velocity profile shown in figure 5-3 is shown in figure 5-4. The turbulence intensity from r/R = 0 to 0.60 has an approximate value of 1.75 percent for all three positions upstream of the impeller. This again indicates very low turbulence levels. The slight increase in turbulence intensity of this region of the flow over that shown in figure 5-2 is likely due to the three-fold increase in Reynolds number. As shown previously in figure 5-2, the turbulence intensity increases from 1.25 percent at r/R = 0.60 to 10 to 11 percent at r/R =

0.95. This would be expected from the developing boundary layer and viscous mixing occurring there and is near the values expected from steady-state fully developed pipe flow.

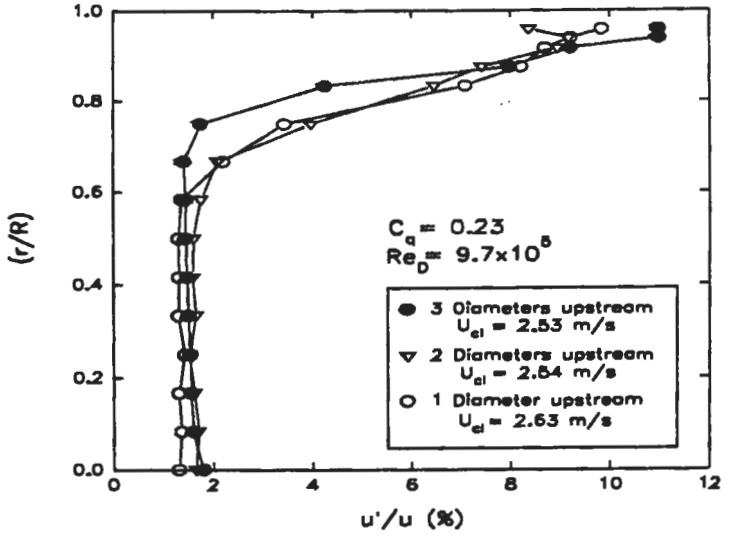

Figure 5-4. Turbulence Intensity for Re_D of 9.7x10^5 and C_q of 0.23

Figure 5-5 shows the mean velocity profiles corresponding to three different flow coefficients at a distance of one pipe diameter upstream of the impeller. The profile for the design C_q of 0.23 is used for reference. It can be seen that the off-design profiles are more skewed with an increase in C_q. As such, the profile for a C_q of 0.40 is the most skewed. The shape of the off-design profiles shows the beginnings of the effect of the impeller tip on the flow field. Despite the irregularities of the off-design flows, they are still uniform from r/R = 0.0 to 0.50.

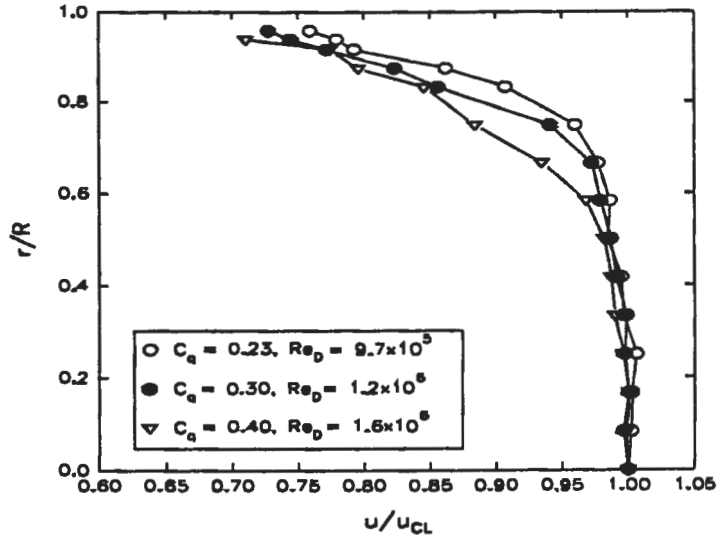

Figure 5-5. u-Component Mean Velocity Profiles for Above Design C_q Flows at One Diameter Upstream of the Impeller

A turbulence intensity plot for the velocity profile shown in figure 5-5 is presented in figure 5-6. This plot shows that the turbulence intensity of all three different C_q velocity profiles is uniform at approximately 1.25 to 1.50 percent from r/R = 0.0 to 0.6; the high off-design C_q flows have turbulence intensity plots that do not vary greatly, if at all, from the design point C_q of 0.23. Similar to the previous presentations of turbulence intensity, there is an increase in turbulence intensity outside the uniform flow region to 10 to 11 percent as r/R approaches a value of one.

A comparison of below-design-point C_q mean velocity profiles at one diameter upstream of the impeller is given in figure 5-7. It is seen that the velocity profile for a C_q of 0.15 does not vary greatly from that of the design C_q of 0.23, where from r/R = 0.0 to 0.70 the flow is uniform within 1 percent. A much greater contrast is seen when one examines the velocity profile with a C_q of 0.10. Here the impeller is operating at such an off-design condition that the pump causes significant recirculation of the flow. A more meaningful representation of the flow field for this impeller operating point can be seen from the time history of the flow at a given point in the flow field, which will be presented later.

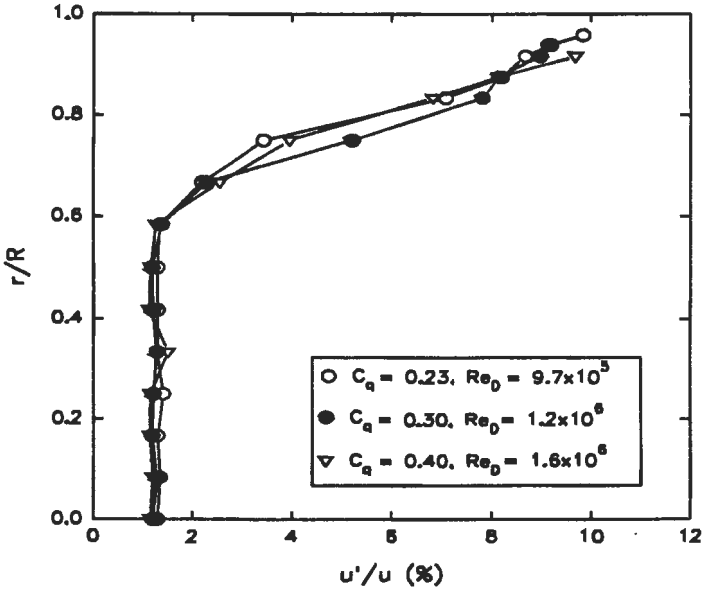

Figure 5-6. Turbulence Intensity for Above Design C_q Flows One Diameter Upstream of the Impeller

Figure 5-8 shows a turbulence intensity plot for the velocity profile presented in figure 5-7. Examination of this plot shows that, although there was little difference between the velocity profiles for flow coefficients of 0.23 and 0.15, there is a distinct difference between the corresponding turbulence intensity profiles. The fluctuations in turbulence intensity for the case of C_q equal to 0.15 are due to unsteady suction side flow separation at the leading edge of the impeller blades. As will be shown later, the flow velocity experiences large cyclic variations, resulting in apparently high turbulence intensity.

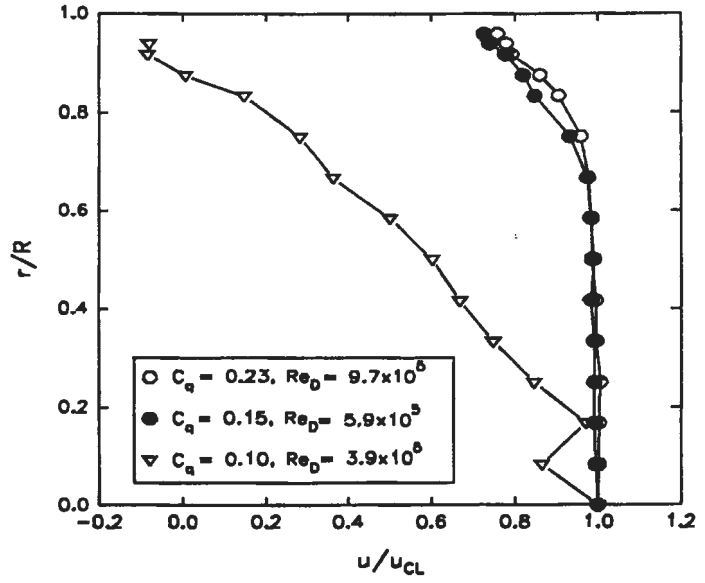

Figure 5-7. u-Component Mean Velocity Profiles for Below Design C_q Flows One Diameter Upstream of the Impeller

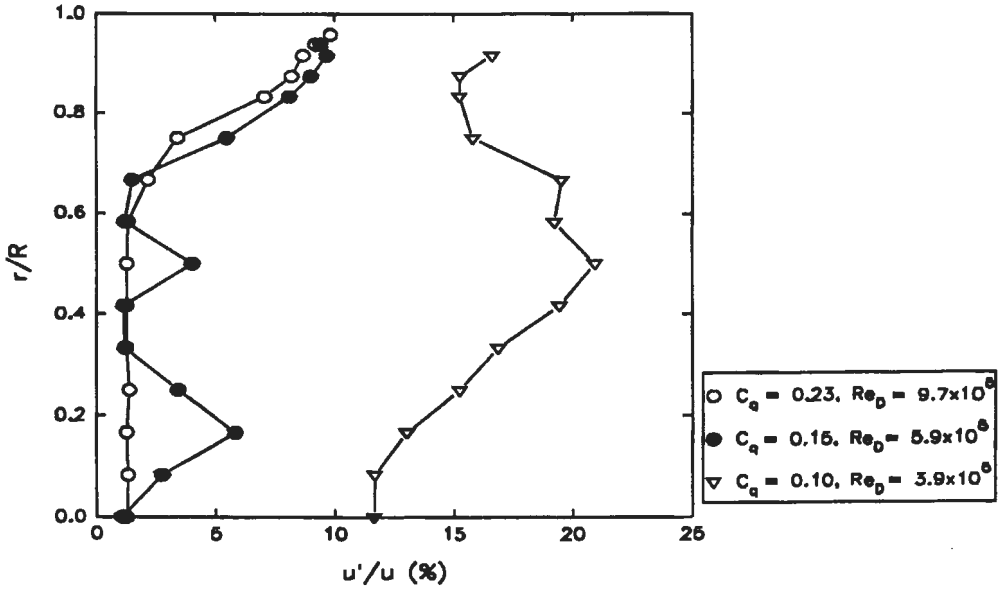

Figure 5-8. Turbulence Intensity for Below Design C_q Flows One Diameter Upstream of the Impeller

For the case of C_q = 0.10, turbulence intensity values are very large, ranging from 10 to 20 percent of the mean flow over the entire profile. This is not a true indication of turbulence intensity but instead is a measure of the flow unsteadiness due to pump surging at low C_q's. This cyclic nature is evident in figures 5-9 and 5-10, which show the time history of the instantaneous u- and v-components at a radial location of r/R = 0.667 and one diameter upstream of the impeller. It can be seen in figure 5-9 that the u-component oscillates from a maximum of

2.29 m/sec to a minimum of -3.66 m/sec. Here the negative velocity denotes reverse flow (i.e., upstream instead of downstream).

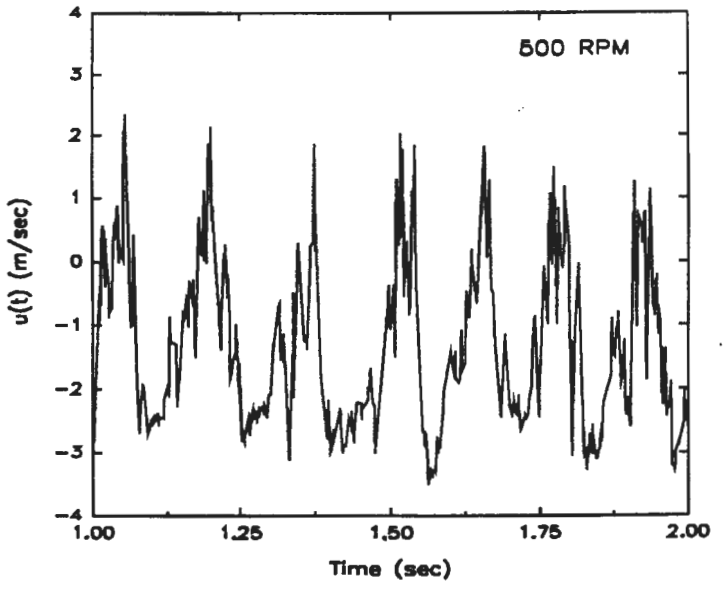

Figure 5-9. u-Component Velocity One Diameter Upstream of Impeller at a C_q of 0.10

Figure 5-10 shows that the v-component of velocity oscillates from a maximum of 5.79 m/sec to a minimum of -3.05 m/sec in the same manner as the u-component. In fact, these two plots show that the u and v-components are coupled and that oscillations occur at approximately 8 Hz. This frequency correlates with the impeller rotational speed of 500 rpm (8.33 rev/sec). It is unknown why there is a correlation with impeller rotation since the flow is asymmetric except for the discharge, which may be the cause of this phenomenon.

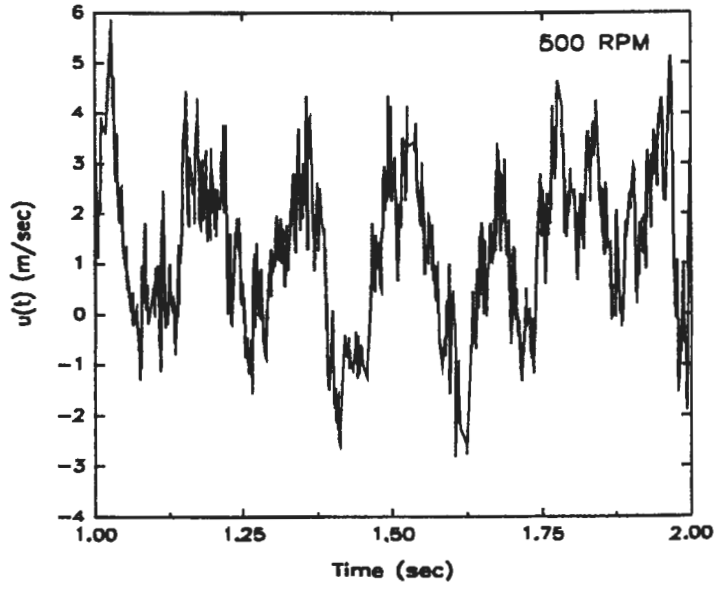

Figure 5-10. v-Component Velocity One Diameter Upstream of Impeller at a C_q of 0.10

COMPARISON OF LDV AND TRANSIENT FLOWMETER FLOW RATES

Figure 5-11 shows a typical velocity profile obtained from the LDV along with its associated curve fit subsequently used for the integration of the profile to determine flow rate through the inlet pipe. Only the portion of the flow that was non-uniform was curve-fit, in order to obtain a more accurate fit. A number of selected profiles were analytically integrated and the results were compared to the corresponding NUWC transient flowmeter output. Table 5-1 shows the results of the velocity profile integrations compared to flowmeter data, along with operating conditions. Percent differences ranged from 2.55 to 6.51 percent. Those values are very small considering the inaccuracy associated with the curve fit and the lack of LDV data near the wall, which accounts for a considerable area of the pipe cross-section. These results provide credibility to both the flowmeter and LDV accuracy statements made in this report.

Table 5-1. LDV - Flowmeter Flow Rate Comparison

Test Number	Flow Coefficient, Cq	Rot. Speed, N (rpm)	Meter Flow Rate l/sec, (gal/min)	Integrated Flow Rate l/sec, (gpm) (LDV)	Percent Difference, %
1	0.23	500	57.4 (910)	58.9 (934)	2.55
2	0.23	1500	172.2 (2730)	184.2 (2919)	6.51
3	0.23	1500	172.2 (2730)	183.0 (2900)	5.90

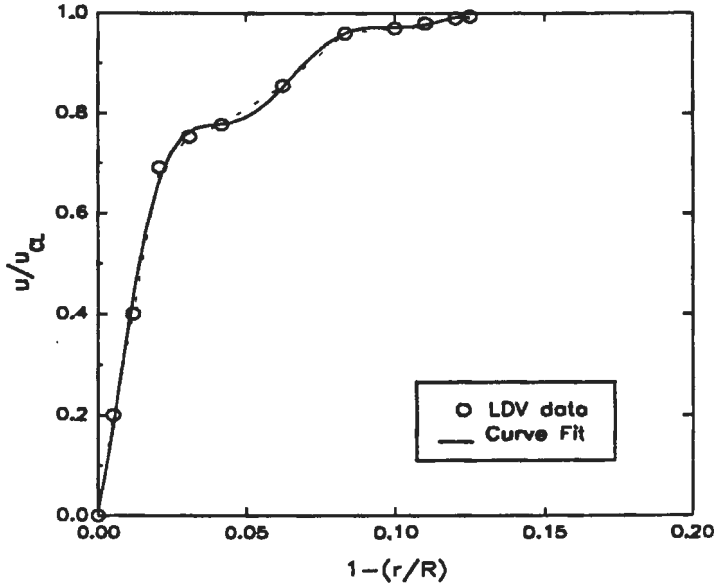

Figure 5-11. Curve-fit of Boundary Layer from Inlet Pipe Velocity Profile

TRANSIENT IMPELLER INLET DATA

As stated previously in section 4, transient time histories were obtained one and two diameters upstream of the impeller nose for radial locations of r/R from 0 to 1. Since velocity profiles obtained at these locations were similar, only one profile is provided. These time histories were used to construct instantaneous velocity profiles across the inlet pipe radius at various instances in time during the transient event. Several typical velocity profiles can be found in figures 5-12 and 5-13. It should be noted that the high acceleration of the transient coupled with the noise generated by scattered light in the pipe made it impossible to acquire data from r/R = 0.0 to 0.175 for these inlet transient tests.

Figure 5-12 shows the velocity profiles for times during the acceleration phase of the transient time history. At t = 0.50 second the velocity during ramp-up is near its maximum with maximum acceleration maintained. This has the effect of surppressing the diffusion of viscosity from the pipe walls into the flow field, preventing the growth of the boundary layer. Thus, the flow maintains its uniformity across the pipe radius. At t = 0.60 second the flow has reached its maximum and remains at an approximately constant flow rate for a short period. It is seen that the boundary has begun to develop slightly beyond r/R = 0.80, but the flow is still within 2.5 percent of uniformity. At t = 0.75 second, the flow is beginning to decelerate. It can be seen that at this point the boundary layer has begun to propagate further into the flow. At t = 1.00 second the flow rate is still high, but with increased deceleration. Here the velocity gradient at the wall is significant. The flow remained uniform within 2 percent from r/R = 0.175 to 0.75, as was the case for t = 0.75 second.

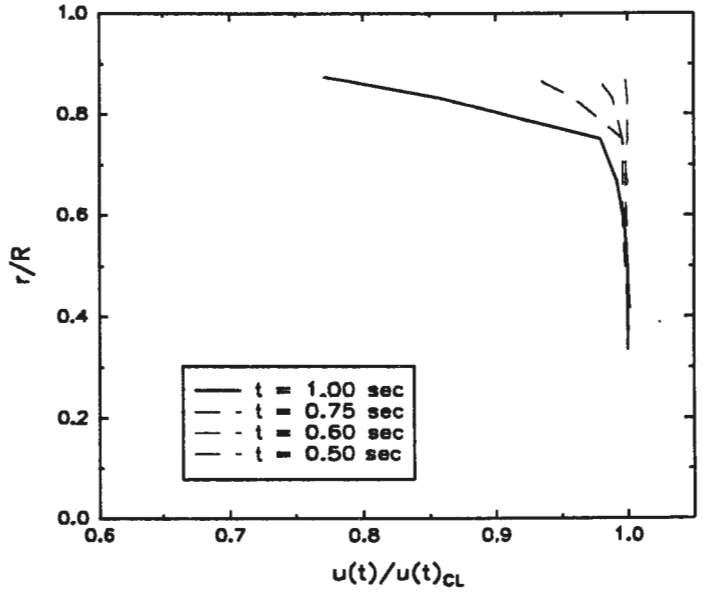

Figure 5-12. u-Component Velocity Profiles of Inlet Pipe Transient up to 1 Second

Figure 5-13 presents velocity profiles during the remainder of the deceleration portion of the transient. The profile at t = 1.00 second, as shown in figure 5-12, is provided for reference.

It can be seen that with continued deceleration of the mean flow, the boundary grows and extends into the flow to as far as r/R = 0.60 at t = 2.00 seconds.

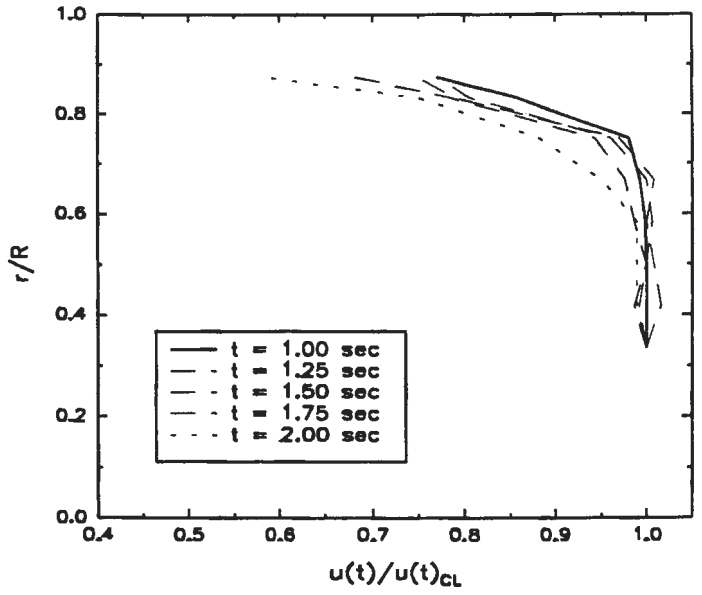

Figure 5-13. u-Component Velocity Profiles of Inlet Pipe Transient from 1.0 to 2.0 Seconds

Figures 5-14 through 5-16 show LDV data acquired at r/R = 0.50, 0.667, and 0.75 compared to transient flowmeter data acquired during the test run. For all three test positions it can be seen that, during the acceleration portion of the transient and prior to the start of deceleration at t = 1.0 second, the LDV and the flowmeter data agree closely. That is expected since the velocity profile is essentially uniform and the local velocity at any radial position should be indicative of the mean cross-sectional velocity. For times beyond 1 second, the LDV data at r/R = 0.5 is higher than the mean from the flowmeter as expected since the velocity was always uniform to that position, and hence has a value greater than the mean. These results validate the stated accuracies for both measurement devices.

Comparison of the transient velocity profiles shown in figures 5-12 and 5-13 and their quasi-steady counterpart at the same C_q is made in figures 5-17 and 5-18.

Figure 5-17 shows an instantaneous velocity profile during the acceleration portion of the transient at a time of 0.5 second with a corresponding C_q of 0.23, which is the subject impeller's design operating point. The steady-state profile for that C_q is also given. This figure most plainly shows the effect of acceleration on the inlet flow field. The steady-state velocity profile shows the expected boundary layer extending to r/R = 0.75 with approximately 1.5 percent uniformity of flow from r/R = 0.75 down to r/R = 0.0. The transient profile shows that the acceleration during the transient ramp-up does indeed restrict boundary layer growth and maintains a uniform flow across the pipe radius. Both profiles shown agree within 1.5 percent where the flow is uniform.

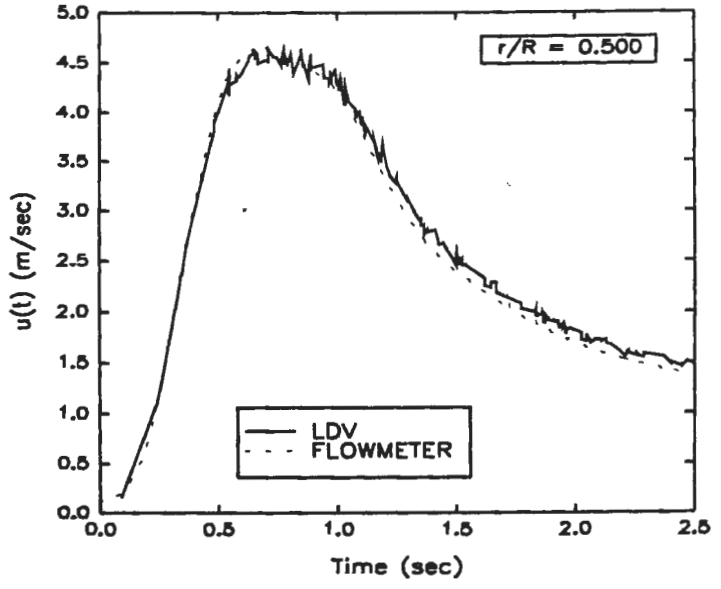

Figure 5-14. Comparison of Flowmeter and LDV Data at r/R = 0.500

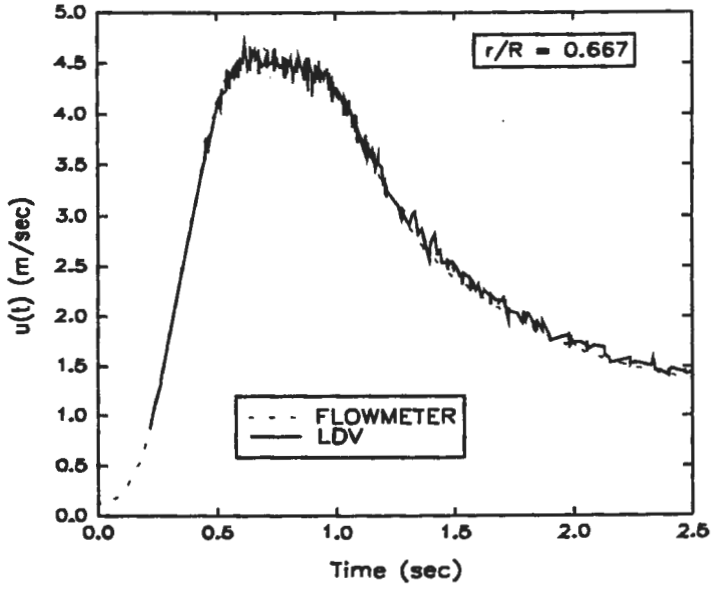

Figure 5-15. Comparison of Flowmeter and LDV Data at r/R = 0.667

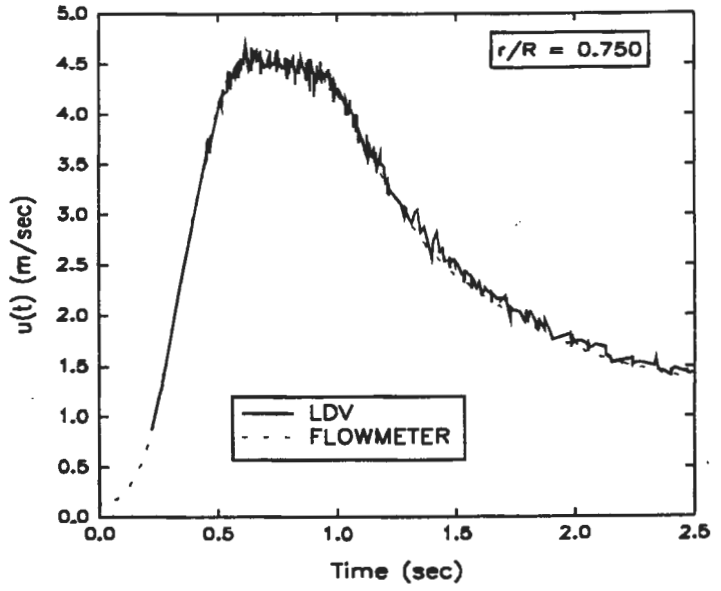

Figure 5-16. Comparison of Flowmeter and LDV Data at r/R = 0.750

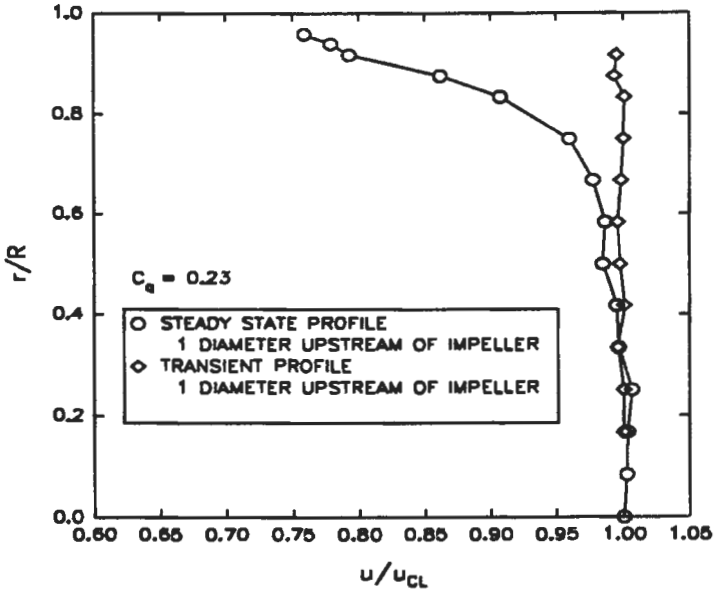

Figure 5-17. u-Component Velocity Profile -
Comparison of Transient and Steady-State Profiles at C_q of 0.23

Figure 5-18 shows the steady-state and transient velocity profiles for a C_q of 0.40; the transient profile occurred at 1.25 seconds and was during deceleration. Here it can be seen that the steady-state profile has a more developed boundary layer relative to the transient profile with uniform flow from only r/R = 0.0 to 0.5. The transient profile appears to be developing toward the steady-state profile, but the stabilizing effects of the earlier acceleration portion are still being felt.

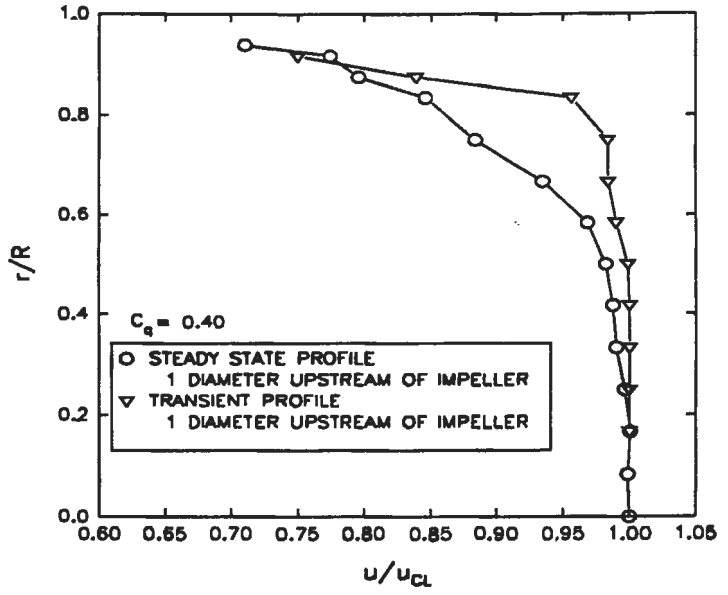

Figure 5-18. u-Component Velocity Profile -
Comparison of Transient and Steady-State Profiles at C_q of 0.40

An ensemble average of the LDV-measured velocity from 20 transient test runs is shown in figure 5-19. These data were acquired at r/R = 0.667, one diameter upstream of the impeller nose. figure 5-19 is similar to Figure 2-9, which was generated from transient flowmeter data. This plot is comparable to the LDV curve of figure 5-15 for a single run but is much smoother due to the averaging.

Figure 5-20 shows the RMS fluctuations versus time curve for the aforementioned 20 runs, non-dimensionalized by the mean velocity. As discussed in Lefebvre and White [5], this curve can be taken as an indication of turbulence intensity throughout the transient if the facility is highly repeatable and the LDV has sufficient accuracy. Comparing figure 5-20 with figure 5-10 for facility repeatability, it appears that from the start of the transient to 0.30 second the high LDV RMS values of greater than 4 percent are attributable to facility non-repeatability. From 0.3 second to the end of the facility controlled portion of the transient at 1.05 seconds, the LDV RMS value averages a low value of approximately 2.5 percent. Since facility repeatability for this time range is less than ±1 percent, either LDV inaccuracy or actual turbulence intensity can be taken as being no greater than 2.5 percent.

STEADY-STATE IMPELLER DISCHARGE DATA

The results of steady-state testing on the impeller discharge flow are shown in figures 5-21 and 5-22. These data were acquired at the axial position x = 0.0 and the radial position r = 38.1 cm (15 in.) from the impeller discharge in order to ensure that the data rate was sufficient for adequate resolution. At this location the data rate was 500 Hz. It was found that the data rate dropped off drastically as the measuring volume was moved toward the impeller. At a radius of 7.6 cm (3 in.) it was found that the noise associated with the beat frequency of the impeller blades, from reflections off the impeller surface, was of a larger magnitude than the Doppler

signal, precluding the ability of the LDV processor to recognize the Doppler and process the data. Consequently, attempts to collect valid data in the inter-blade regions of the impeller flow field as well as near the impeller tip did not yield adequate data rates. Furthermore, adequate data resolution could only be obtained at distances beyond r = 28 cm (11 in.). For this steady-state test, the impeller was operated at a low speed to determine if there was any correlation between velocity and impeller rotational position.

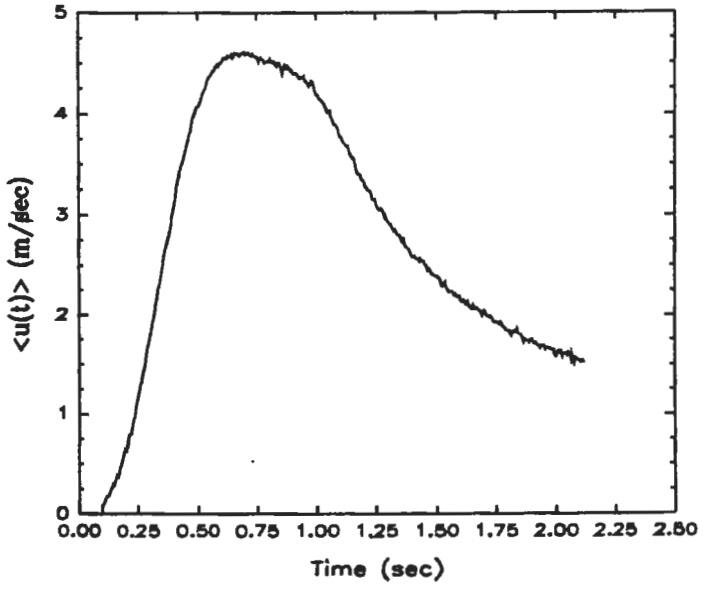

Figure 5-19. Ensemble-Averaged Inlet Pipe LDV Velocity Time History from 20 Repeat Runs

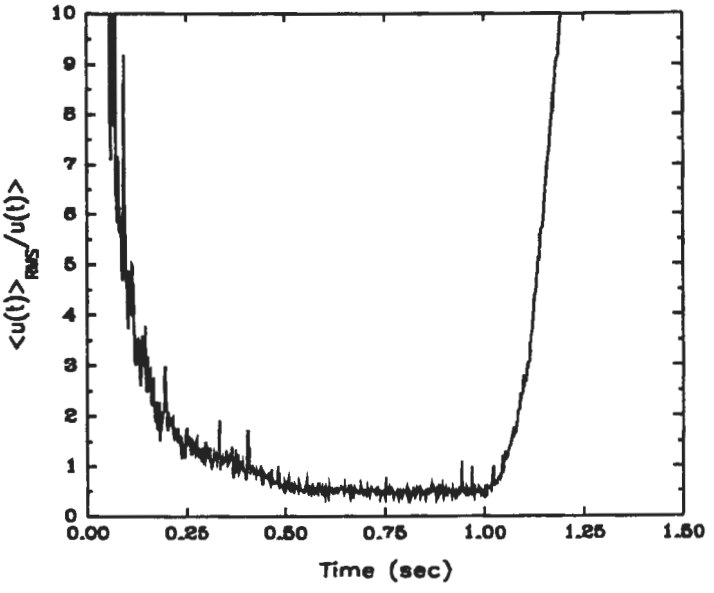

Figure 5-20. $\langle u(t)_{RMS}/u(t)\rangle$ versus Time for Ensemble-Averaged LDV Velocity Time History

Figure 5-21 gives tangential fluid velocity and impeller position time histories from t = 0.0 to 1.50 seconds. Zero degrees impeller position is when the pressure side of the discharge tip of one impeller blade is in the same horizontal plane as the center of the LDV measuring volume. It can be seen that there appears to be some periodicity to the flow on the order of two times the impeller rotational frequency of 2 Hz. The oscillatory nature of the data suggests that there is a high level of circulatory-type flow within the test section. There doesn't appear to be any correlation between velocities at the test point and the impeller's rotational position due to the distance from the impeller.

Figure 5-22 shows similar tangential fluid velocity and impeller position time histories, but from t = 1.50 to 3.00 seconds. Examination of this plot shows that the periodicity on the order of 4 Hz that was seen in figure 5-21 is no longer present. This reveals that the circulatory flow patterns in the test section are of a highly unsteady, random nature. As in the case of figure 5-21 the distance of the test location from the impeller does not allow for correlation with impeller position and the data appear to follow no constant pattern. Examination of the velocity profiles at all four axial locations showed that there was no difference in the profiles.

In an effort to increase data rate, a TSI IFA 650 LDV processor, which is based on new-technology, high-speed signal processing circuitry, was demonstrated by TSI representatives. Data rates at r = 38.1 cm were quadrupled relative to that obtained with the IFA 550. Also, data rates up to 100 Hz were obtained at the impeller discharge. Those rates could have been improved if more time was available for optimizing the flow seeding. Any future tests to obtain more flow detail will require the use of the new processor.

TRANSIENT IMPELLER DISCHARGE DATA

The results of transient discharge testing are presented in figures 5-23 through 5-25. These data are from the r = 28-cm (11-in.) position. The data from this radial position were used since that was the closest position to the impeller at which a reasonable data rate was obtained. Again, the problems with reflections off the impeller surface prohibited data collection near the impeller. Additionally, when the measuring volume was very close to the impeller discharge, the LDV IFA 550 processor could not track the high rate of change of velocity due to its internal phase-lock-looping circuitry, as will be explained below. An attempt was made to eliminate the reflection problem by utilizing flourescein particles as the seeding medium. Flourescein emits in the red wavelengths when illuminated with green light. A red pass optical filter was adapted to the LDV fiberoptic probe so that the only light received by the probe was the light emitted from the seeding particles, effectively blocking out the light reflected off the impeller. This setup was tried and did not yield any improvement in data rate, so the original setup was used.

Figure 5-23 gives the tangential velocity, flow rate, and impeller rotational speed time histories for a transient from t = 0.0 to 1.25 seconds, which is the time of interest as stated in section 2. The data were acquired at r = 28 cm (11 in.) and x = -3.18 cm (-1.25 in.).

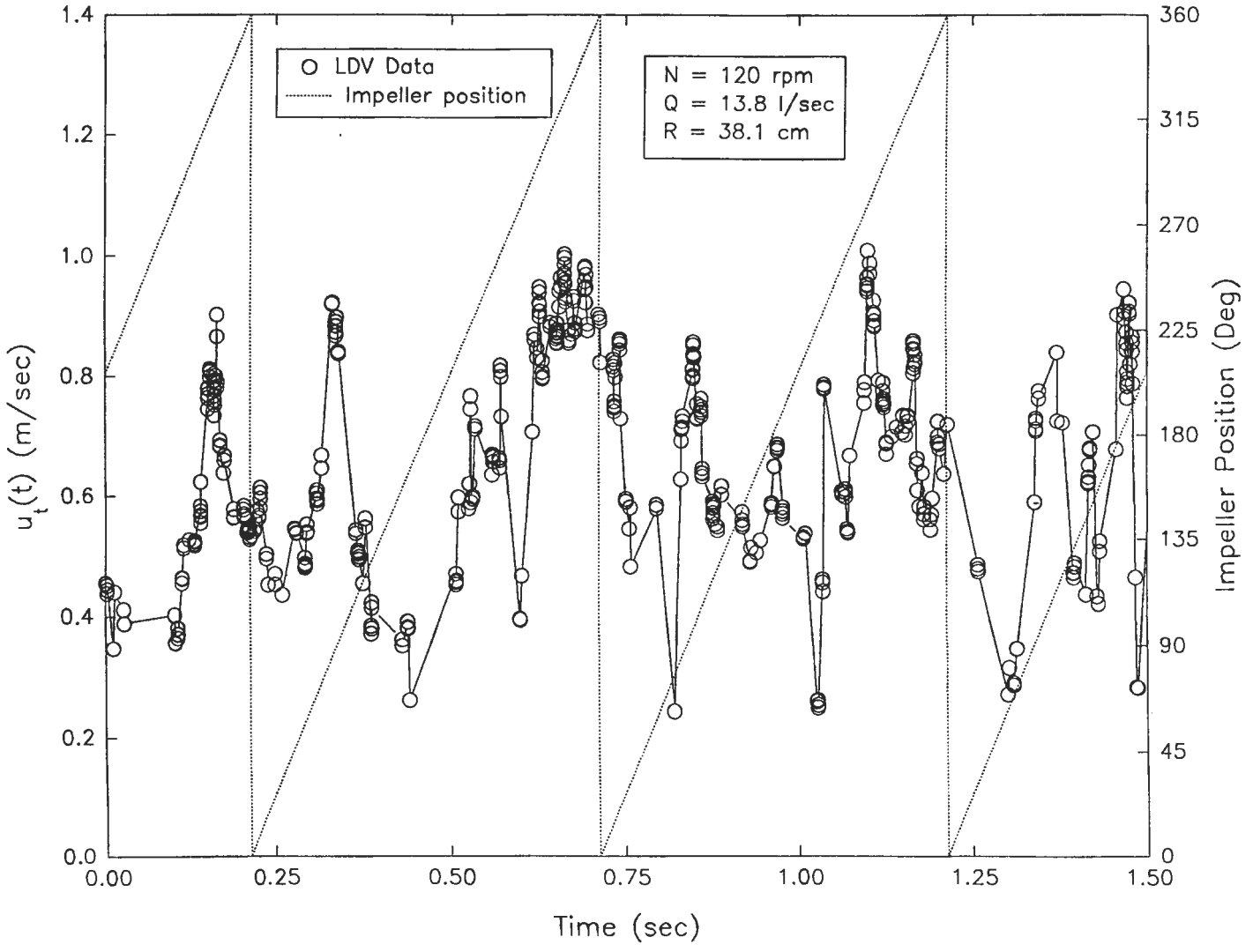

Figure 5-21. Steady-State Tangential Fluid Velocity and Impeller Rotational Position Time Histories from 0.0 to 1.5 Seconds

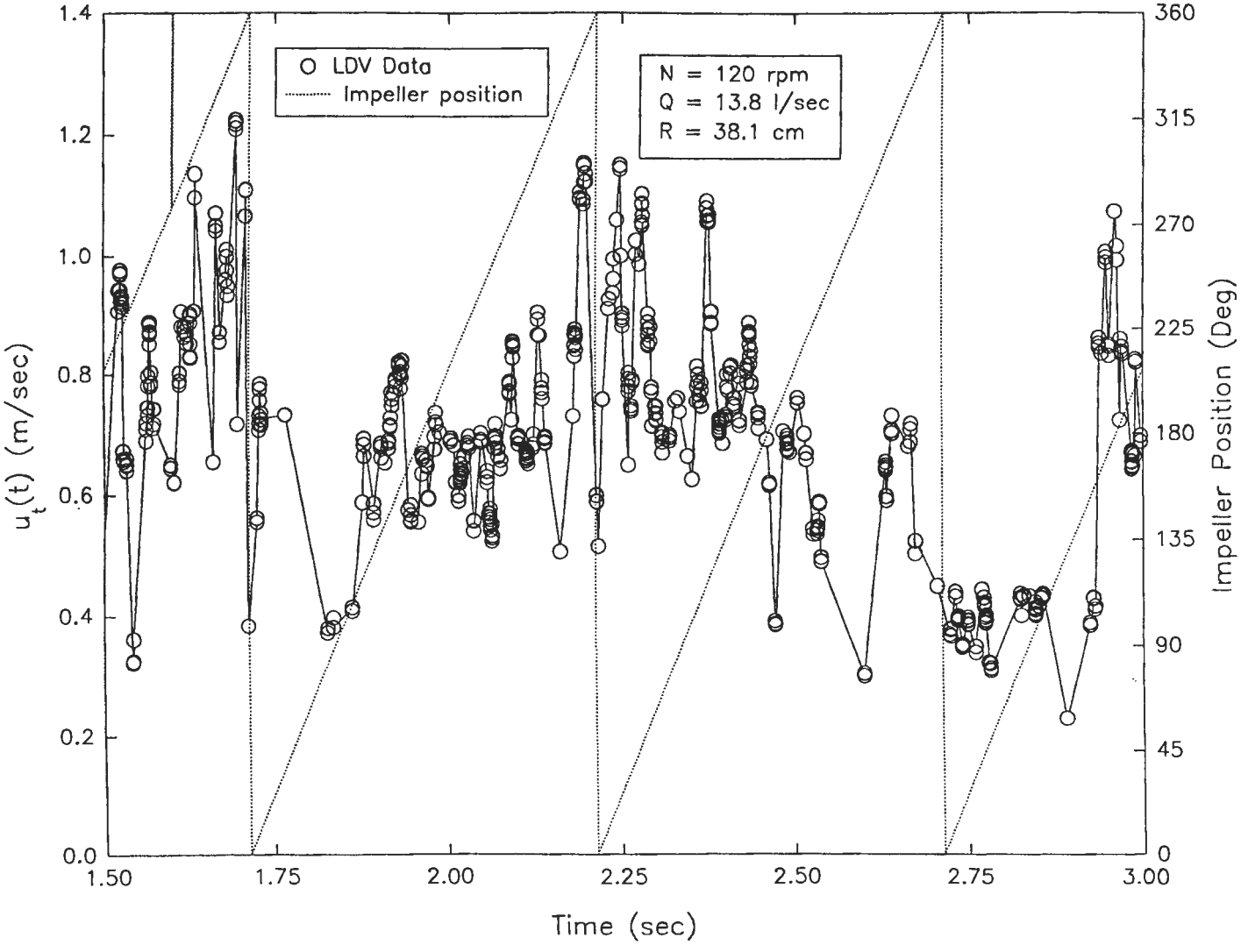

Figure 5-22. Steady-State Tangential Fluid Velocity and Impeller Rotational Position Time Histories from 1.5 to 3.0 Seconds

The overall shape of the $u_t(t)$ curve follows the Q curve; however, the velocity history shows large fluctuations on the order of 15 m/sec peak-to-peak. These fluctuations appear to be due to unsteady circulatory flow in the test section, as was discussed for figures 5-21 and 5-22. The N and Q time histories are given for reference.

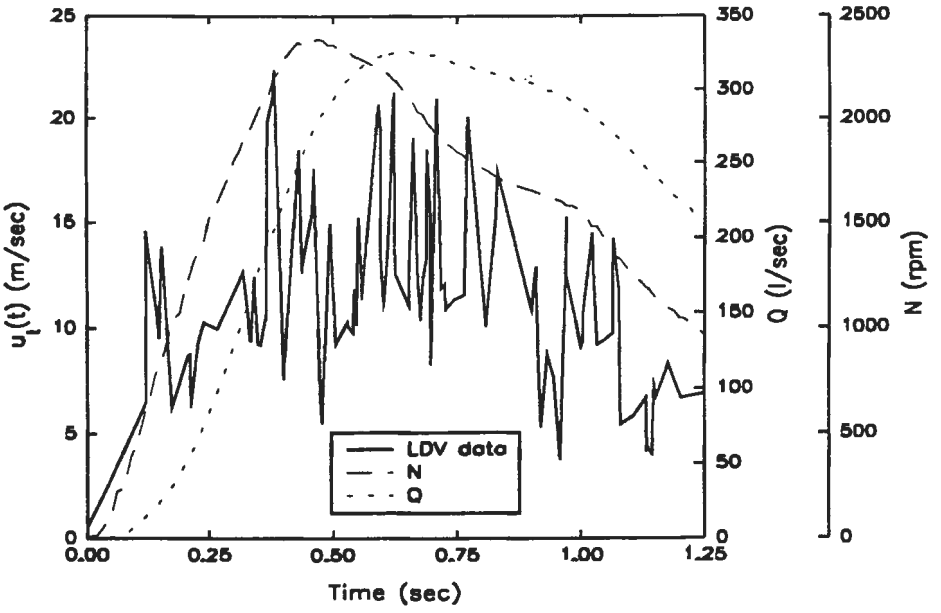

Figure 5-23. Discharge Tangential Fluid Velocity, Flow Rate, and Impeller Rotational Speed for a Transient

Figure 5-24 gives an expanded view of the time histories of tangential fluid velocity at r = 28 cm and x = 0.0 cm along with impeller rotational position for a transient run from t = 0.30 to 0.85 second. This plot shows the lack of sufficient data during the beginning of the transient. It can be seen that from t = 0.30 to 0.50 second there were approximately 18 valid data points for 7 complete rotations of the impeller. The data symbols have been provided to show the reader that the flow is in fact oscillating in the manner seen in figure 5-23. The lack of data at the beginning of the transient can be attributed in part to the phase-lock-looping algorithm used by the IFA 550 processor to validate a data point. In this scheme, a data point is checked against the previous point to determine if it is within 20 percent of the preceding point. If it is not, the point is discarded and the process is repeated for the next point sampled. Due to the high velocity gradient during the initial stages of the transient, the IFA 550 cannot lock onto the flow quickly enough to validate the rapidly changing velocity. Hence, the low data rate at this point.

Figure 5-25 shows the tangential fluid velocity and impeller position time histories for the same transient as figure 5-24, but from t = 0.85 to 1.35 seconds. Here the velocity has reached a maximum with peaks in the oscillations of approximately 20 m/sec peak-to-peak. Once again it is seen that the flow is indeed oscillating during the transient due to the unsteady circulation occurring in the test section at this axial location. Even though the data rate for this portion of the transient is substantially higher than the earlier portion, there is still no way to make a correlation between velocity observed at this point and impeller blade position.

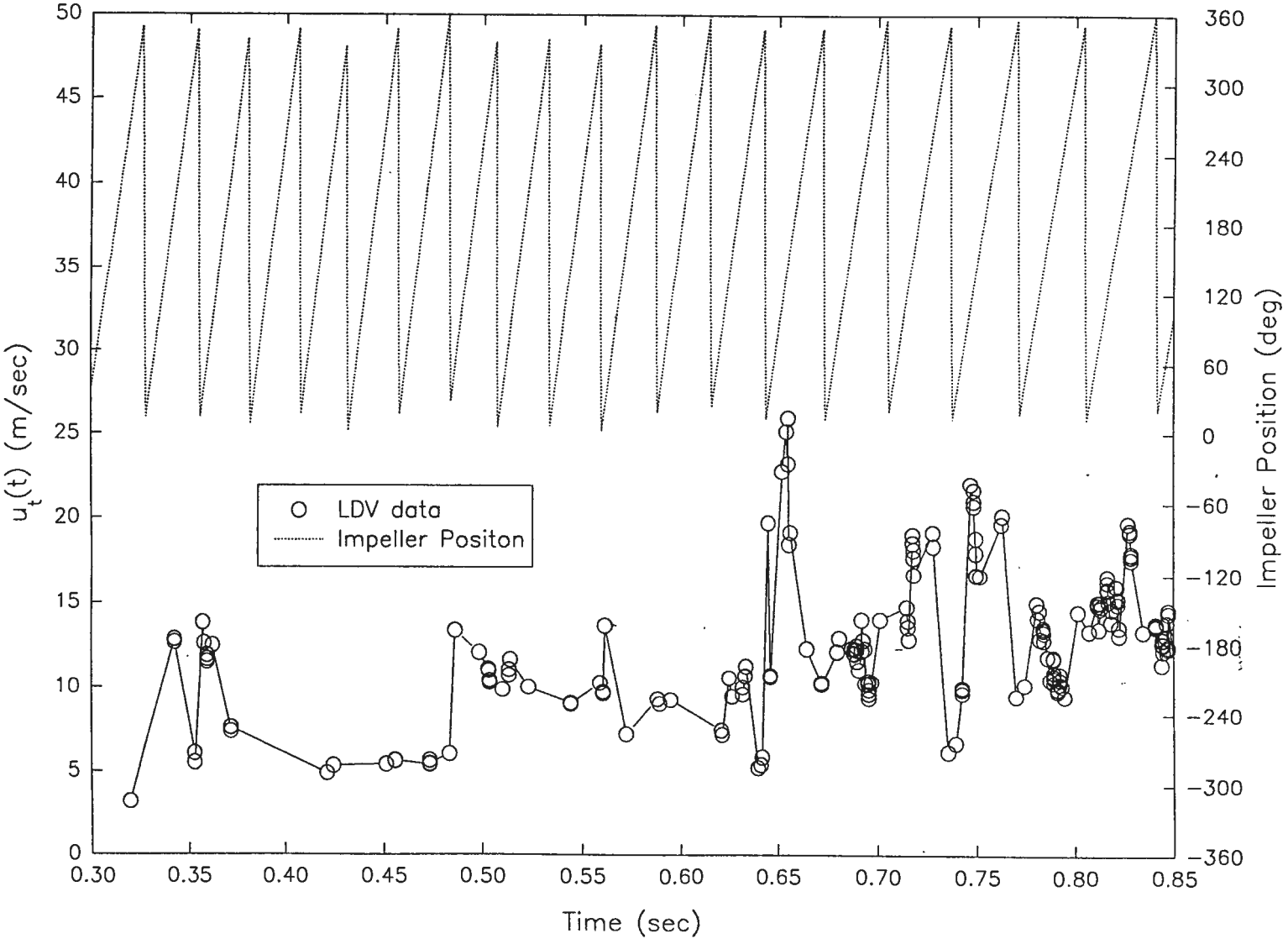

Figure 5-24. Transient Tangential Fluid Velocity and Impeller Rotational Position Time Histories from 0.30 to 0.85 Seconds

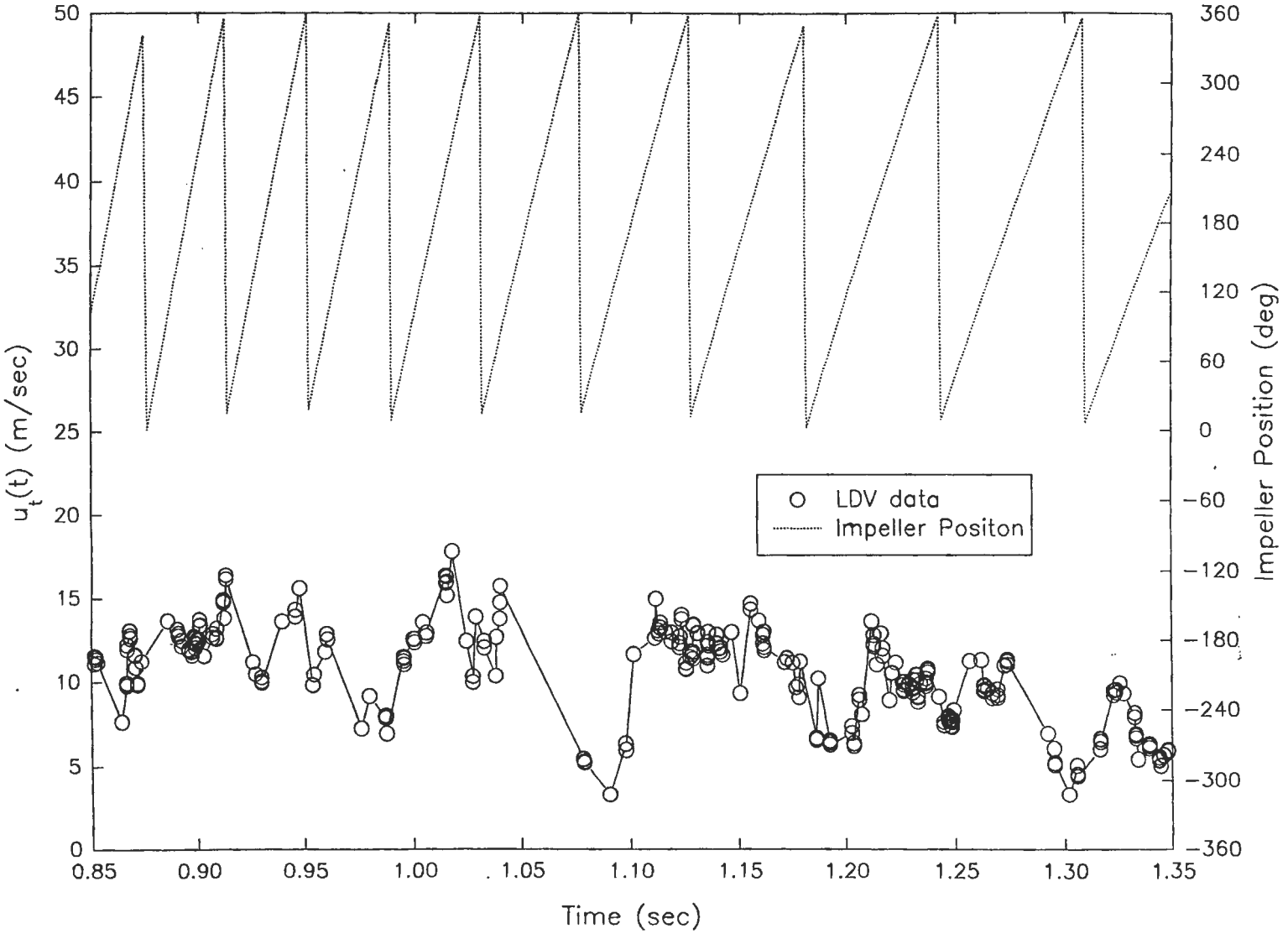

Figure 5-25. Transient Tangential Fluid Velocity and Impeller Rotational Position Time Histories from 0.85 to 1.35 Seconds

TRANSIENT IMPELLER HYDRODYNAMIC PERFORMANCE

Figure 5-26 shows the hydrodynamic performance of the pump impeller typical of the rpm and flow rate versus time histories used for the LDV examinations. Both transient and quasi-steady head coefficients, C_h, as well as rpm, flow rate, and head were plotted versus time for a transient event. These parameters characterize pump performance critical to weapons launch applications. As dictated by the input control N and Q time-histories, the peak flow rate was 321 l/sec (5130 gal/min) and the peak impeller rotational speed was 2400 rpm. Maximum head output was 49 m (160 ft). The difference seen between the transient and quasi-steady C_h curves was discussed previously in section 1 and is further documented in Lefebvre and Barker [1]. For this transient there is a 37 percent difference between head predicted by the quasi-steady and transient C_h curves.

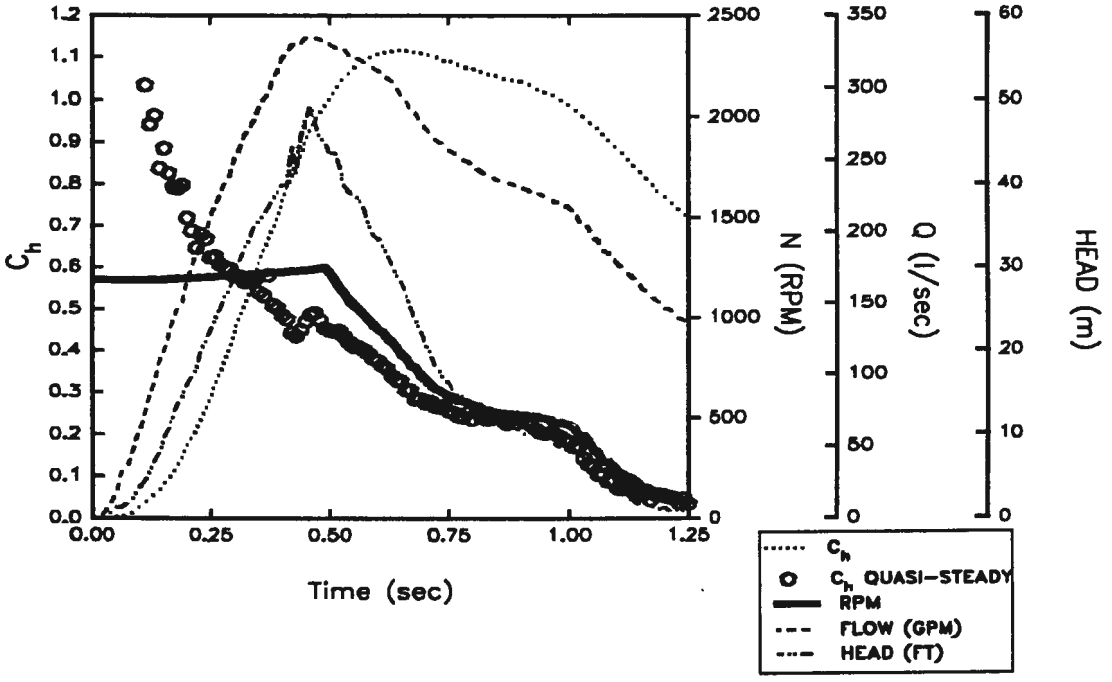

Figure 5-26. Transient Impeller Hydrodynamic Performance

6. CONCLUSIONS

Based on the results presented in this report, the main conclusions are as follows:

1. Facility repeatability during most of the transient is ±1 percent or better, allowing for ensemble averaging of data.

2. Actual transient hydrodynamic performance , based on pressure rise across the impeller, differs from that predicted by quasi-steady theory by up to 37 percent.

3. During steady-state impeller operation:

   a. Inlet velocity profiles were not as developed as those for fully developed pipe flow due to the short length of inlet pipe between the impeller and the flow management section. This was intentional to simulate expected ship conditions.

   b. The turbulence intensity in the inlet pipe was measured by the LDV to be 1.25 percent. Since that value is at the limits of the accuracy of the LDV, the actual turbulence intensity may be lower.

   c. There were significant fluctuations in the inlet flow at low off-design C_q's during steady-state operation. Fluctuations were not observed during transient operation due to the short time the flow was at these low C_q's.

4. During the transient:

   a. The instantaneous inlet pipe velocity profiles are essentially uniform across the pipe diameter up to the time that peak Q was reached. This was the result of the retardation of viscous effects due to the stabilizing effects of acceleration.

   b. Immediately following deceleration of the transient, enhanced diffusion resulted in boundary layer development into the flow. The velocity profiles continued to develop throughout the remainder of the transient; however, they never reached their quasi-steady equivalent.

   c. During most of the transient, inlet pipe turbulence intensity at a radial location of r/R = 0.667 was less than 2.5 percent. Since this was at the limits of LDV accuracy, the actual turbulence intensity may be lower.

5. Unsteady circulatory flow patterns in the test section, uncorrelated with impeller rotational position, were observed in both steady-state and transient discharge results.

6. Unavoidable reflections off the impeller surface during discharge testing resulted in decreased SNR as the measuring volume was moved toward the impeller. Adequate data rates could be achieved only at a minimum radial distance of 28 cm (11 in.) from the impeller discharge tip.

7. REFERENCES

1. P.J. Lefebvre and W.P. Barker, "Evaluation of Transient Effects on 1/3 Scale Model Submarine Launch Pump Impellers," NUSC Technical Report 7032, Naval Underwater Systems Center, Newport, RI, 1 August 1991 (UNCLASSIFIED).

2. P.J. Lefebvre, W.P. Barker, and R.G. Gregory, "Evaluation of Cavitation Effects on Transiently Operating 1/3 Scale Model Submarine Launch Pump Impellers"(U), NUWC Technical Memorandum 922011A, Naval Undersea Warfare Center Division, Newport, RI, 15 October 1992 (CONFIDENTIAL).

3. R.G. Gregory, P. J. Lefebvre, and W. P. Barker," Design, Operation, and Evaluation of the NUWC Transient Impeller Test Facility," NUWC Technical Memorandum 922000, Naval Undersea Warfare Center Division, Newport, RI, 2 January 1992 (UNCLASSIFIED).

4. P.J. Lefebvre and W.W. Durgin, "A Transient Electromagnetic Flowmeter and Calibration Facility," *Journal of Fluids Engineering*, March 1990.

5. P.J. Lefebvre and F.M.White, "Detailed Measurement of Accelerating - Flow Properties in Pipes," A.S.M.E., FED - Vol. 139, 1992.

DISTRIBUTION LIST

External

CNR(ONR 1132F (P. Purtell), ONR 23 (J. Fein), ONR 233 (G. Remers, R. Vogelsong))

CDNSWC (Codes 0114 (L.Becker), 15 (W. Morgan), 15 (W. Blake),15 42(J. Gorsky, Y.T. Lee), 2720 (T. Bein))

NAVSEA (SEA-05W13)
SEAWOLF PROGRAM MANAGER (PMS-350T1)

Internal

Codes 0251
0261
0262 (2)
02242
10
22
38
3891
411 (C. Wagner)
80
8092
81
82
83
832
8321
8323
833
8302
8321 (W. Barker, J. Little, M. Ansay)
8322 (P. Lefebvre (3), R. Gregory, J. Gutkowski)

Total: 40